NeuroImage: Clinical 28 (2020) 102504

Contents lists available at ScienceDirect

NeuroImage: Clinical

journal homepage: www.elsevier.com/locate/ynicl

# Tau PET and relative cerebral blood flow in dementia with Lewy bodies: A PET study

E.E. Wolters [a,b,*], M. van de Beek [b], R. Ossenkoppele [b,c], S.S.V. Golla [a], S.C.J. Verfaillie [a], E. M. Coomans [a], T Timmers [a,b], D. Visser [a], H. Tuncel [a], F. Barkhof [a,d], R. Boellaard [a], A. D. Windhorst [a], W.M. van der Flier [b,e], Ph. Scheltens [b], A.W. Lemstra [b], B.N.M. van Berckel [a]

[a] Department of Radiology & Nuclear Medicine, Amsterdam Neuroscience, Vrije Universiteit Amsterdam, Amsterdam UMC, Amsterdam, The Netherlands
[b] Alzheimer Center Amsterdam, Department of Neurology, Amsterdam Neuroscience, Vrije Universiteit Amsterdam, Amsterdam UMC, Amsterdam, The Netherlands
[c] Clinical Memory Research Unit, Lund University, Lund, Sweden
[d] Institutes of Neurology & Healthcare Engineering, UCL, London, United Kingdom
[e] Department of Epidemiology and Biostatistics, Vrije Universiteit Amsterdam, Amsterdam UMC, Amsterdam, The Netherlands

ARTICLE INFO

*Keywords:*
Tau
Relative cerebral blood flow
FDG PET
Dementia with Lewy bodies
Cognition

ABSTRACT

*Purpose:* Alpha-synuclein often co-occurs with Alzheimer's disease (AD) pathology in Dementia with Lewy Bodies (DLB). From a dynamic [$^{18}$F]flortaucipir PET scan we derived measures of both tau binding and relative cerebral blood flow (rCBF). We tested whether regional tau binding or rCBF differed between DLB patients and AD patients and controls and examined their association with clinical characteristics of DLB.

*Methods:* Eighteen patients with probable DLB, 65 AD patients and 50 controls underwent a dynamic 130-minute [$^{18}$F]flortaucipir PET scan. DLB patients with positive biomarkers for AD based on cerebrospinal fluid or amyloid PET were considered as DLB with AD pathology (DLB-AD+). Receptor parametric mapping (cerebellar gray matter reference region) was used to extract regional binding potential ($BP_{ND}$) and $R_1$, reflecting (AD-specific) tau pathology and rCBF, respectively. First, we performed regional comparisons of [$^{18}$F]flortaucipir $BP_{ND}$ and $R_1$ between diagnostic groups. In DLB patients only, we performed regression analyses between regional [$^{18}$F]flortaucipir $BP_{ND}$, $R_1$ and performance on ten neuropsychological tests.

*Results:* Regional [$^{18}$F]flortaucipir $BP_{ND}$ in DLB was comparable with tau binding in controls ($p > 0.05$). Subtle higher tau binding was observed in DLB-AD+ compared to DLB-AD- in the medial temporal and parietal lobe (both $p < 0.05$). Occipital and lateral parietal $R_1$ was lower in DLB compared to AD and controls (all $p < 0.01$). Lower frontal $R_1$ was associated with impaired performance on digit span forward (standardized beta, st$\beta = 0.72$) and category fluency (st$\beta = 0.69$) tests. Lower parietal $R_1$ was related to lower delayed (st$\beta = 0.50$) and immediate (st$\beta = 0.48$) recall, VOSP number location (st$\beta = 0.70$) and fragmented letters (st$\beta = 0.59$) scores. Lower occipital $R_1$ was associated to worse performance on VOSP fragmented letters (st$\beta = 0.61$), all $p < 0.05$.

*Conclusion:* The amount of tau binding in DLB was minimal and did not differ from controls. However, there were DLB-specific occipital and lateral parietal relative cerebral blood flow reductions compared to both controls and AD patients. Regional rCBF, but not tau binding, was related to cognitive impairment. This indicates that assessment of rCBF may give more insight into disease mechanisms in DLB than tau PET.

## 1. Introduction

Dementia with Lewy Bodies (DLB) is clinically characterized by cognitive decline, visual hallucinations, parkinsonism, fluctuating cognition/ alertness and rapid eye movement (REM) sleep behavior disorder (RBD) (McKeith et al., 2017). The pathological hallmark of DLB is the presence of cortical Lewy Bodies, which are neuronal inclusions of alpha-synuclein proteins (Kosaka, 1978). Concomitant Alzheimer's disease (AD) pathology, i.e. amyloid plaques and neurofibrillary tangles (NFT), are present in more than 70% of the autopsied DLB-cases (Dugger et al., 2014; Howlett et al., 2015; Irwin et al., 2017). AD pathology in patients with DLB is associated with faster disease progression and

* Corresponding author at: Department of Radiology & Nuclear Medicine, Amsterdam UMC, location VUmc, PO Box 7057, 1007MB Amsterdam, The Netherlands.
*E-mail address:* ee.wolters@amsterdamumc.nl (E.E. Wolters).

https://doi.org/10.1016/j.nicl.2020.102504
Received 11 June 2020; Received in revised form 8 November 2020; Accepted 10 November 2020
Available online 19 November 2020

higher burden of alpha-synuclein pathology (Howlett et al., 2015; Irwin et al., 2017, 2018; Lemstra et al., 2017). Therefore, *in-vivo* identification of coinciding AD pathology may be important in a clinical setting.

The tau PET tracer [$^{18}$F]flortaucipir may serve as an *in-vivo* marker for AD specific tau pathology in DLB. [$^{18}$F]flortaucipir binds with high affinity to paired helical filaments of AD tau, exhibits low affinity to tau in non-AD tauopathies (Marquie et al., 2017) and does not bind to alpha-synuclein protein depositions (Lowe et al., 2016; Marquie et al., 2015). Previous [$^{18}$F]flortaucipir PET studies in DLB have shown inconsistent spatial patterns of cortical uptake, but in general lower retention levels than in AD (Gomperts et al., 2016; Kantarci et al., 2017; Lee et al., 2018; Mak et al., 2019; Nedelska et al., 2019; Ossenkoppele et al., 2018; Smith et al., 2018a). Furthermore, some studies showed a relationship between AD tau pathology and cognitive functioning or disease severity (Gomperts et al., 2016; Smith et al., 2018b), while others have not (Kantarci et al., 2017; Lee et al., 2018).

Thus, the contribution of AD tau pathology to the symptomatology of DLB is currently unclear, likely reflecting a dependency on other additional pathologies. Since there are no validated alpha-synuclein PET tracers available (Kotzbauer et al., 2017), the contribution of alpha-synuclein cannot be assessed directly. Therefore, more general imaging measurements such as changes in cerebral blood flow, which can serve as a surrogate marker for neuronal activity, may be of additional value in DLB. DLB is characterized by occipital hypoperfusion, which has been demonstrated with arterial spin labeling brain magnetic resonance imaging (MRI) (Binnewijzend et al., 2014; Fong et al., 2011; Nedelska et al., 2018; Taylor et al., 2012), single photon emission computerized tomography (SPECT) (Colloby et al., 2002; Goto et al., 2010; Hanyu et al., 2006; Ishii et al., 1999; Lobotesis et al., 2001; Pasquier et al., 2002) and PET (Rodell et al., 2016).

A dynamic [$^{18}$F]flortaucipir PET allows for exact quantification of tau binding, but also the measurement of the relative cerebral blood flow (rCBF), which is expressed by $R_1$. $R_1$ represents the ratio between $K_1$ (the rate constant for the exchange of the tracer from blood to tissue) in the target tissue and the reference region. $R_1$ and 2-[$^{18}$F]-fluoro-2-doxy-D-glucose (FDG) PET metabolism are closely related (Ottoy et al., 2019; Peretti et al., 2019; Rodriguez-Vieitez et al., 2016) and clinical characteristics have been associated with hypometabolism in DLB (Morbelli et al., 2019). We hypothesize that $R_1$ as a marker of rCBF is also related to the clinical core features and cognitive impairment in DLB.

Therefore, our first objective was to determine the regional patterns of tau PET and rCBF in DLB compared to AD and controls using a single dynamic [$^{18}$F]flortaucipir PET scan. Secondly, we explored the influence of AD pathology, measured in cerebrospinal fluid (CSF) or with amyloid PET, on the amount of [$^{18}$F]flortaucipir PET binding in DLB. Finally, we assessed the relationship between tau binding and rCBF with the clinical core criteria of DLB and cognitive impairment.

## 2. Methods

### 2.1. Recruitment of participants

We included 133 subjects from the Amsterdam Dementia Cohort (van der Flier and Scheltens, 2018) of whom 18 were diagnosed with dementia with Lewy bodies (DLB, n = 11) or mild cognitive impairment with Lewy Bodies (MCI-LB, n = 7). As reference group, we included 65 amyloid positive symptomatic AD patients (MCI-AD (n = 13), AD (n = 52)) and 50 controls with subjective cognitive decline (SCD).

All subjects underwent a standardized dementia screening, including medical history, extensive neuropsychological assessment, physical and neurological examination, lumbar puncture, blood tests, electroencephalography and MRI. Diagnosis was established by consensus in a multidisciplinary meeting (van der Flier and Scheltens, 2018).

#### 2.1.1. DLB

DLB patients met clinical diagnostic consensus criteria for probable DLB (DEM-LB) (McKeith et al., 2017) or MCI-LB (i.e. two or more core clinical features, with only one impaired cognitive domain and no interference in activities in daily living) (McKeith et al., 2020; van de Beek et al., 2020). The diagnosis of DLB was supported by [$^{123}$I]FP-CIT SPECT (DAT-SPECT) findings showing presynaptic dopaminergic deficits (available for 13 individuals). DLB patients with positive CSF biomarkers for AD (i.e. total tau (t-tau)/Aβ42 fraction > 0.52 (Duits et al., 2014), and/or a positive amyloid ([$^{11}$C] Pittsburgh compound B or [$^{18}$F] florbetaben) PET scan by visual assessment (de Wilde et al., 2017; Zwan et al., 2014) were considered as DLB with AD pathology (DLB-AD+). CSF biomarkers were available for 15 DLB patients and amyloid ([$^{11}$C]PiB n = 1 and [$^{18}$F]florbetaben n = 6) PET scans were available for 7 DLB patients. In total, 6 DLB patients were DLB-AD+ and 12 were DLB-AD-.

#### 2.1.2. AD

The diagnosis of MCI-AD and AD met core clinical criteria (Albert et al., 2011; McKhann et al., 2011) according to the National Institute on Aging and Alzheimer's Association (NIA-AA) and all had positive CSF biomarkers (i.e. t-tau/Aβ42 fraction > 0.52 (Duits et al., 2014) and/or a positive Aß ([$^{11}$C]PiB or [$^{18}$F]florbetaben) PET scan by visual assessment (de Wilde et al., 2017; Zwan et al., 2014). We excluded distinct clinical variants of AD such as posterior cortical atrophy (Crutch et al., 2012), logopenic variant primary progressive aphasia (Gorno-Tempini et al., 2011), cortical basal syndrome (Armstrong et al., 2013) and behavioural/ dysexecutive variants (Ossenkoppele et al., 2015), since these clinical variants show typically a different tau PET uptake pattern than the typical AD cases (Ossenkoppele et al., 2016).

#### 2.1.3. Controls

We included controls with SCD from the SCIENCe project (Slot et al., 2018). SCD is defined as self-reported cognitive complaints, but without any objective impairment in performance on cognitive or neurological tasks or brain damage as evidenced by MRI. Controls with evidence of substantial amyloid pathology after visual reading of $SUVR_{50\text{-}70}$ of [$^{18}$F] florbetapir amyloid PET scans (Golla et al., 2018a) and/ or positive CSF biomarkers (i.e. t-tau/Aβ42 fraction > 0.52 (Duits et al., 2014)), were classified as amyloid positive subjects. We included all controls (irrespective of their amyloid status) for the primary analysis and as a secondary analysis we only included amyloid negative controls.

Exclusion criteria for all participants were (1) significant cerebrovascular disease on MRI (e.g. territorial infarct), (2) major traumatic brain injury, (3) major psychiatric or neurological disorders other than AD and DLB (4) current substance abuse. The study protocol was approved by the Medical Ethics Review Committee of the Amsterdam UMC, location VU Medical center.

All procedures were in accordance with the ethical standards Medical Ethics Review Committee of the Amsterdam UMC and with the 1964 Helsinki declaration and its later amendments or comparable ethical standards. Informed consent was obtained from all individual participants included in the study.

### 2.2. Imaging acquisition

All participants underwent a single dynamic 130 min [$^{18}$F]flortaucipir PET scan on a Philips Ingenuity TF-64 PET/CT scanner. The scanning protocol consisted of two dynamic PET acquisitions of 60 and 50 min respectively, with a 20-minute break in between (Golla et al., 2017; Wolters et al., 2018). The first 60 min dynamic acquisition started simultaneously with a bolus injection 237 ± 13 MBq [$^{18}$F]flortaucipir (injected mass 1.13 ± 0.82 μg). The second PET acquisition was co-registered to the first dynamic PET scan using (Volume Imaging in Neurological Imaging) Vinci software (Vollmar et al., 2002). PET list mode data were rebinned into a total of 29 frames (1 × 15, 3 × 5, 3 × 10, 4 × 60, 2 × 150, 2 × 300, 4 × 600 and 10 × 300 seconds).

Ten DLB patients additionally underwent a static [$^{18}$F]FDG PET scan on the same scanner as the [$^{18}$F]flortaucipir PET scan (Philips Ingenuity TF-64 PET/CT scanner). Scans were performed under standard resting conditions with eyes closed. The [$^{18}$F]FDG PET scan was performed within 4 months of the [$^{18}$F]flortaucipir PET scan (median: 22 days, range 8–113 days). All subjects fasted at least four hours before tracer injection, and plasma glucose levels were measured before the scan. Following a low-dose CT scan, a 15-min static emission scan was acquired from 45 min after injection of [$^{18}$F]FDG. PET list mode data were rebinned into a total of 3 frames (3 × 300 seconds).

All subjects underwent 3D-T1 weighted and FLAIR scans on a 3.0 Tesla MR scanner (Ingenuity TF PET/MR, Philips Medical Systems, Best, The Netherlands).

### 2.3. Imaging processing

Data from all PET scans were reconstructed using 3D RAMLA with a matrix size of 128 × 128 × 90 and a final voxel size of 2 × 2 × 2 mm$^3$, including standard corrections for dead time, decay, attenuation, randoms and scatter. The 3D-T1 MR images were co-registered to the averaged images (frame 8 – 29 ([$^{18}$F]flortaucipir); frame 1–3 ([$^{18}$F]FDG PET)) of the PET scan using Vinci software (Vollmar et al., 2002) in native space. Cortical gray matter regions of interest (ROIs, Hammers template (Hammers et al., 2003)) were subsequently delineated on the MR images and superimposed on the PET scan using PVElab (Svarer et al., 2005). [$^{18}$F]flortaucipir binding potential ($BP_{ND}$) and $R_1$ images, reflecting AD tau pathology and rCBF respectively, were generated using receptor parametric mapping (RPM) (Golla et al., 2018b). We used cerebellar gray matter as a reference region, which we previously validated for both $BP_{ND}$ and $R_1$ using RPM (Golla et al., 2018b, 2017). [$^{18}$F]FDG SUVr images were generated by normalizing the uptake to the mean value of the cerebellum (grey matter).

The following bilateral ROIs were created *a priori* (Visser et al., 2020) based on the Hammers atlas (Hammers et al., 2003): medial temporal (hippocampus, parahippocampal and ambient gyri, medial anterior temporal lobe), lateral temporal (superior temporal gyrus, middle and inferior temporal gyri), medial parietal (posterior cingulate), lateral parietal (inferolateral parietal lobe, superior parietal gyrus), occipital (cuneus, lingual gyrus, lateral occipital lobe) and frontal (middle frontal gyrus, orbitofrontal gyri, superior frontal gyrus) regions.

For voxel-wise analyses, using Statistical Parametric Mapping (SPM) version 12 software (Wellcome Trust Center for Neuroimaging, University College London, UK), we warped all native space parametric $BP_{ND}$ and $R_1$ images to Montreal Neurological Institute (MNI) space, by using the transformation matrixes derived from warping the co-registered T1-weighted MRI scans to MNI space. Warped images were visually checked for transformation errors.

### 2.4. Cognition

The Mini-Mental State Examination (MMSE) was used as a measure of global cognitive status (Folstein et al., 1975) across diagnostic groups.

### 2.5. Education

Education was rated using the Dutch Verhage scoring system. This system uses a 7-point scale, ranging from 'primary education not finished' (1), to 'master's degree' (7), applied on the Dutch education system (Verhage, 1964).

### 2.6. Clinical characteristics of DLB

#### 2.6.1. Cognition

We additionally used the following cognitive tests for DLB patients: Dutch version of the Rey Auditory Verbal Learning Test (RAVLT) immediate recall and delayed recall, Digit span Forward, Trial Making Test [TMT] version A, Digit span Backward, TMT version B, letter fluency test (D-A-T), category fluency version animals and two tests of visual object and space perception (VOSP) battery: number location and fragmented letters. TMT were inverted so that lower scores indicated worse performance. All individual cognitive tests were transformed into *Z* scores, using the mean and SD of the equivalent test from an independent cognitively normal reference group (n = 553, 60 ± 10 years, 54% female, MMSE = 29 ± 1) (Groot et al., 2018).

#### 2.6.2. Core clinical features

The core clinical features of DLB were assessed using standardized methods. Parkinsonism was assessed by a trained medical doctor, using the motor subscale of the Unified Parkinson's disease rating scale (UPDRS, range 0–108) (Goetz et al., 2008). Visual hallucinations were determined with the Questionnaire on Psychotic Experiences (Rossell et al., 2019). We rated visual hallucinations as present when patients experienced visual hallucinations in the past month. Fluctuating cognition was assessed using the Clinical Assessment of Fluctuations (CAF) (Walker et al., 2000). We rated fluctuations as present when one of the two screening questions was answered positively. REM sleep behavior disorder (RBD) was assessed with the screening question of the Mayo Sleep Questionnaire (Boeve et al., 2011). We rated RBD as present if caregivers noticed enactment of dreams on three or more occasions.

### 2.7. Statistical analyses

#### 2.7.1. Total group

To assess group differences at baseline, univariate analysis of variance (ANOVA) and $\chi^2$ were performed where appropriate. First, we compared differences in regional $BP_{ND}$ and $R_1$ values across six ROIs between diagnostic groups using ANOVA and show uncorrected (*) and corrected for multiple comparisons (6 ROIs × 3 diagnostic groups) using Bonferroni (#). We report the differences between diagnostic groups with and without correction of age and sex. Second, voxel-wise comparisons for $BP_{ND}$ and $R_1$ between the diagnostic groups using SPM12 were performed. Analyses were adjusted for age and sex; a p-value < 0.001 (uncorrected for multiple comparisons) was considered statistically significant. Third, we performed receiver operating characteristic (ROC) area-under-the-curve (AUC) analyses to investigate whether regional [$^{18}$F]flortaucipir $BP_{ND}$ or $R_1$ could discriminate DLB from AD or controls.

#### 2.7.2. DLB

First, to investigate whether amyloid PET or an AD-like CSF biomarker signature may have influenced [$^{18}$F]flortaucipir $BP_{ND}$, we used an analysis of covariance (ANCOVA) model with age and sex as covariates and AD pathology as fixed factor (DLB-AD+ vs DLB-AD-). Second, to explore the influence of disease stage on the amount of [$^{18}$F]flortaucipir $BP_{ND}$ and $R_1$, we used an ANCOVA model with age and sex as covariates and dementia stage (MCI-LB vs. DEM-LB) as fixed factor. Third, linear regression analyses, adjusted for age, sex and education, were performed to investigate associations between [$^{18}$F]flortaucipir $BP_{ND}$ or $R_1$ (independent variables) and individual cognitive test performances (dependent variables). We report the level of significance both with and without correction for multiple comparisons (six ROIs * ten cognitive tests) using Bonferroni. Fourth, for the associations between [$^{18}$F]flortaucipir $BP_{ND}$ or $R_1$ (independent variables) with clinical core criteria of DLB, linear regression analyses (for continuous dependent variables; UPDRS) and logistic regressions (for binary [i.e. yes/no] dependent variables; parkinsonism, fluctuations, hallucinations and RBD), adjusted for age and sex, were performed. We repeated this analysis by replacing [$^{18}$F]flortaucipir $BP_{ND}$ for [$^{18}$F]flortaucipir SUVr and [$^{18}$F]flortaucipir $R_1$ for [$^{18}$F]FDG SUVr.

Although rCBF is tightly coupled to [$^{18}$F]FDG hypometabolism, there are differences in spatial overlap (Ottoy et al., 2019; Peretti et al., 2019; Rodriguez-Vieitez et al., 2016). To further examine the relations

between rCBF and hypometabolism, we performed a (exploratory) linear regression analysis between [$^{18}$F]flortaucipir $R_1$ (independent variable) and [$^{18}$F]FDG SUVr (dependent variable) within a subset with both modalities available (n = 10).

A $p$ value $< 0.05$ was considered statistically significant. Analyses were performed using R (version 3.5.3, R Development Core Team 2019).

For all linear regressions, standardized beta's (sβ) were used as an outcome variable. By standardizing all variables in the equation, we obtain an easy interpretable outcome measure, which is comparable across regressions. The sβ is the change in the outcome variable for 1 standard deviation in change of the predictor. All sβ's are tested against the null hypothesis that a sβ of 0 yields no effect (Landis, 2005).

## 3. Results

### 3.1. Demographics

Demographic and clinical characteristics of the total sample and per diagnostic group are presented in Table 1. Diagnostic groups did not differ in age, sex and education. As expected, MMSE score was lower for both DLB and AD patients compared to controls. Of the DLB patients, 33% (n = 6) had evidence of AD pathology (measured with CSF / amyloid PET).

**Table 1**
Overview of demographics, [$^{18}$F]flortaucipir $BP_{ND}$ and $R_1$.

| | DLB (n = 18) | AD (n = 65) | Controls (n = 50) |
|---|---|---|---|
| Age (years) | 69(6) | 66(8) | 66(8) |
| Sex (female/male) | 3/15 | 30/35 | 24/26 |
| No. Aβ positive subjects | 6(33%) *¥ | 65(100%) *† | 20(40%) |
| No. FP-CIT SPECT abnormal | 100% (n = 13) | – | – |
| Education (Dutch Verhage scale) | 5[3–7] | 6[3–7] | 6[2–7] |
| MMSE | 25(4) *† | 24(3) *† | 29(1) |
| Timelag (months) between MRI to [$^{18}$F]flortaucipir | 0 (0 – 2) | 0(-5 – 5) | 0 (-14 – 12) |
| [$^{18}$F]flortaucipir $BP_{ND}$ | | | |
| Medial temporal | 0.01(0.08) *#¥ | 0.23 (0.17)*#† | −0.01(0.11) |
| Lateral temporal | 0.09(0.06) *#¥ | 0.43(0.31) *#† | 0.07(0.09) |
| Medial parietal | 0.08(0.07) *#¥ | 0.48(0.39) *#† | 0.09(0.09) |
| Lateral parietal | 0.04(0.05) *#¥ | 0.46(0.42) *#† | 0.07(0.09) |
| Occipital | 0.07(0.04) *#¥ | 0.37(0.36) *#† | 0.10(0.07) |
| Frontal | 0.02(0.05) *#¥ | 0.23(0.30) *#† | −0.01(0.06) |
| [$^{18}$F]flortaucipir $R_1$ | | | |
| Medial temporal | 0.69(0.04) *# † | 0.68(0.06) *† | 0.66(0.03) |
| Lateral temporal | 0.84(0.06) *#† | 0.87(0.08) *† | 0.90(0.05) |
| Medial parietal | 0.99(0.08) | 0.97(0.11) *#† | 1.04(0.07) |
| Lateral parietal | 0.81(0.06) *#¥ † | 0.87(0.10) *#† | 0.94(0.06) |
| Occipital | 0.90(0.06) *#¥,† | 0.98(0.09) *#† | 1.02(0.05) |
| Frontal | 0.88(0.05) | 0.89(0.07) | 0.88(0.05) |
| Clinical core criteria DLB | | | |
| Visual hallucinations, No. (%) | 5(30%) | | |
| Fluctuations, No. (%) | 15(83%) | | |
| Parkinsonism, No. (%) | 16(89%) | | |
| RBD, present No. (%) | 11(61%) | | |

Mean (SD) are reported for all variables, except sex (nfemale/nmale), and time lag education (median [minimum–maximum]). Differences in demographic, clinical characteristics between disease groups were assessed using ANOVA for continuous variables .and $\chi^2$ for dichotomous data.
*Significantly different from controls†, AD subjects¥ at $p_{uncorrected} < 0.05$.
# Significantly different from controls†, AD subjects¥ at $p_{Bonferroni} < 0.05$ (corrected for 3 × 6 comparisons).

### 3.2. [$^{18}$F]flortaucipir $BP_{ND}$ images

Mean [$^{18}$F]flortaucipir $BP_{ND}$ images showed visually minimal tau binding in the inferior lateral temporal lobe in DLB, which was comparable to the uptake pattern observed in controls and substantially less pronounced than the widespread and intense pattern of tau binding in AD (Fig. 1). We explored the influence of AD pathology, measured with amyloid PET or an AD-like CSF, on the amount of [$^{18}$F]flortaucipir $BP_{ND}$ in DLB by examining regional differences in tau binding. Visually, subtle higher tau binding was observed in DLB-AD+ compared to DLB-AD- (supplementary Fig. 1) and regional analyses showed higher tau binding in the medial temporal (0.06 vs −0.01) and medial parietal lobe (0.13 vs 0.06) for DLB-AD+ patients vs DLB-AD- (both $p < 0.05$, supplementary Table 1).

### 3.3. Regional differences in [$^{18}$F]flortaucipir $BP_{ND}$ and $R_1$ across diagnostic groups

Fig. 2 shows the regional [$^{18}$F]flortaucipir $BP_{ND}$ and $R_1$ values across diagnostic groups. Uncorrected results showed that across all ROIs, [$^{18}$F]flortaucipir $BP_{ND}$ was lower in DLB (e.g. occipital $BP_{ND}$; 0.07 ± 0.04) compared to AD (0.37 ± 0.36, $p_{Bonferroni} < 0.05$) and comparable with controls (0.10 ± 0.07, $p > 0.05$) (Table 1 and Fig. 2). Occipital and lateral parietal $R_1$ was lower in DLB (e.g. occipital $R_1$; 0.90 ± 0.06) compared to both AD (0.98 ± 0.09) and controls (1.02 ± 0.05), all $p_{Bonferroni} < 0.05$ (Table 1 and Fig. 2). When age and sex were added as covariates, results remained essentially the same, with the exception of differences between DLB vs. AD for the lateral parietal $R_1$ (supplementary Table 2).

### 3.4. Voxel-wise differences in [$^{18}$F]flortaucipir $BP_{ND}$ and $R_1$ across diagnostic groups

Voxel-wise comparisons showed lower [$^{18}$F]flortaucipir $BP_{ND}$ in the temporoparietal and occipital lobe (supplementary Fig. 2) and lower occipital [$^{18}$F]flortaucipir $R_1$ in DLB compared to AD (Fig. 3). Compared to the regional analyses, a more widespread lower parietal-temporal-occipital [$^{18}$F]flortaucipir $R_1$ pattern was observed in DLB compared to controls (Fig. 3). There were no regions showing higher [$^{18}$F]flortaucipir $BP_{ND}$ or $R_1$ in DLB compared to AD or controls.

### 3.5. Discriminative accuracy of [$^{18}$F]flortaucipir $BP_{ND}$ and $R_1$ across diagnostic groups

ROC curves for [$^{18}$F]flortaucipir $BP_{ND}$ and $R_1$ for distinguishing DLB from AD and controls are presented in Fig. 4. For DLB vs AD, discriminative accuracy was higher for [$^{18}$F]flortaucipir $BP_{ND}$ than for $R_1$ (Fig. 4, A, C). [$^{18}$F]flortaucipir $BP_{ND}$ could best discriminate DLB from AD in the medial (AUC = 0.88 [CI = 0.81 – 0.96]) and lateral (AUC = 0.88 [CI = 0.81 – 0.95]) temporal lobe (Fig. 4, A). In comparison, discriminative accuracy of [$^{18}$F]flortaucipir $R_1$ was highest the occipital lobe (AUC = 0.77 [CI = 0.65 – 0.88], Fig. 4, C).

[$^{18}$F]flortaucipir $R_1$ better distinguished DLB from controls compared to $BP_{ND}$ (Fig. 4, B, D). [$^{18}$F]flortaucipir $R_1$ showed highest discriminative accuracy in the lateral parietal (AUC=0.94 [CI = 0.88 – 1]) and occipital lobe (AUC = 0.94 [CI = 0.88 – 0.99]) for DLB vs controls (Fig. 4, D). For $BP_{ND}$, the frontal lobe (AUC = 0.69[CI = 0.55 – 0.83]) was the most discriminating region for DLB vs controls (Fig. 4, B).

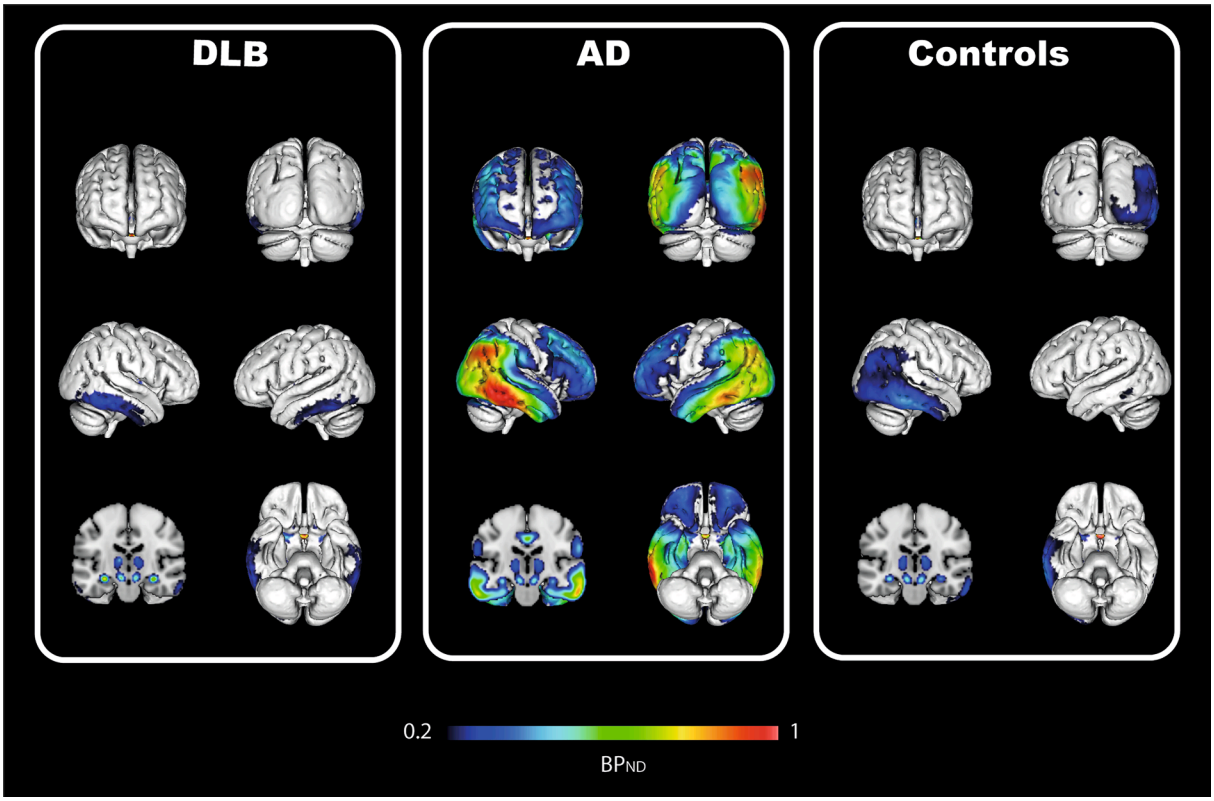


**Fig. 1.** Mean [$^{18}$F]flortaucipir parametric $BP_{ND}$ images for Dementia with Lewy bodies (DLB), Alzheimer's disease (AD) and controls.

### 3.6. Associations of [$^{18}$F]flortaucipir $BP_{ND}$ and $R_1$ with clinical characteristics in DLB

We first explored the influence of disease stage on the amount of [$^{18}$F]flortaucipir $BP_{ND}$ and $R_1$ within DLB. We found no significant differences between $BP_{ND}$ and/or $R_1$ for MCI-LB vs. DEM-LB (supplementary Table 3). Next, we examined whether $BP_{ND}$ and/ or $R_1$ is associated with clinical characteristics of DLB, i.e. signs of Parkinsonism, fluctuations, hallucinations and RBD, as well as cognitive decline measured with ten neuropsychological tests.

Binary logistic regression models showed no associations between [$^{18}$F]flortaucipir $BP_{ND}$ or $R_1$ and Parkinsonism, fluctuations, hallucinations and RBD (all $p > 0.05$). There were no associations between [$^{18}$F]flortaucipir $BP_{ND}$ and any of the cognitive tests (all $p > 0.05$) within DLB. However, there were several associations between [$^{18}$F]flortaucipir $R_1$ and cognitive test scores (Fig. 5). Lower frontal $R_1$ was associated to worse performance on the digit span forward ($st\beta = 0.72$, $p = 0.01$) and category fluency ($st\beta = 0.69$, $p < 0.01$) tests. Lower medial parietal $R_1$ was related to lower scores on delayed recall ($st\beta = 0.50$, $p = 0.04$) and VOSP number location ($st\beta = 0.70$, $p = 0.03$). Lower lateral parietal $R_1$ was associated with lower immediate recall ($st\beta = 0.48$, $p = 0.03$) and VOSP fragmented letters ($st\beta = 0.59$, $p = 0.03$) scores. Lower occipital $R_1$ was associated to worse performance on VOSP fragmented letters ($st\beta = 0.61$, $p = 0.03$). These associations did not survive Bonferroni correction for multiple comparisons (all $p > 0.05$).

### 3.7. Associations of [$^{18}$F]flortaucipir SUVr with clinical characteristics in DLB

When we repeated our analysis and replaced [$^{18}$F]flortaucipir $BP_{ND}$ for [$^{18}$F]flortaucipir SUVr, we found comparable results (supplementary Table 4), i.e. there were no associations between [$^{18}$F]flortaucipir SUVr and Parkinsonism, fluctuations, hallucinations, RBD, UPDRS or cognitive test scores (all $p > 0.05$)

### 3.8. [$^{18}$F]FDG SUVr

Within a subset of DLB patients with both modalities available (n = 10), we explored whether [$^{18}$F]flortaucipir $R_1$ and [$^{18}$F]FDG SUVr were spatially related. [$^{18}$F]FDG SUVr and $R_1$ parametric images had substantial overlap (Fig. 6, panel A). Lower [$^{18}$F]flortaucipir $R_1$ was strongly related to lower [$^{18}$F]FDG SUVr in the lateral temporal ($st\beta = 0.89$), lateral parietal ($st\beta = 0.92$), occipital ($st\beta = 0.90$) and frontal ($st\beta = 0.82$, all $p < 0.01$) lobe, with exception of the medial temporal and medial parietal lobe, both $p > 0.05$ (Fig. 6, panel B).

Next, we examined whether [$^{18}$F]FDG SUVr is associated with clinical characteristics of DLB. Binary logistic regression models showed no associations between [$^{18}$F]FDG SUVr and Parkinsonism, fluctuations, hallucinations and RBD (all $p > 0.05$). However, there were several associations between regional [$^{18}$F]FDG SUVr and cognitive test scores (MMSE, digit span forward /backward, immediate recall, category / letter fluency; supplementary Fig. 4).

## 4. Discussion

We used a single dynamic [$^{18}$F]flortaucipir PET scan to simultaneously quantify tau PET and rCBF and examined regional differences in these measures between DLB patients and AD patients and controls. We found minimal tau binding, but region-specific rCBF reductions compared to AD and controls. We observed lower occipital rCBF in DLB, and rCBF values in this region accurately distinguished DLB from AD and controls. Tau PET was not related to clinical core features (parkinsonism, fluctuations, hallucinations and RBD) and cognitive impairment, but lower parietal and frontal rCBF were associated with worse performance on a variety of cognitive tests. Taken together, these results indicate that in our sample AD tau pathology contributed only minimally to the symptoms of DLB and that rCBF measurements may be more clinically meaningful than tau PET in DLB.

One of our main results is that we found little tau binding in DLB

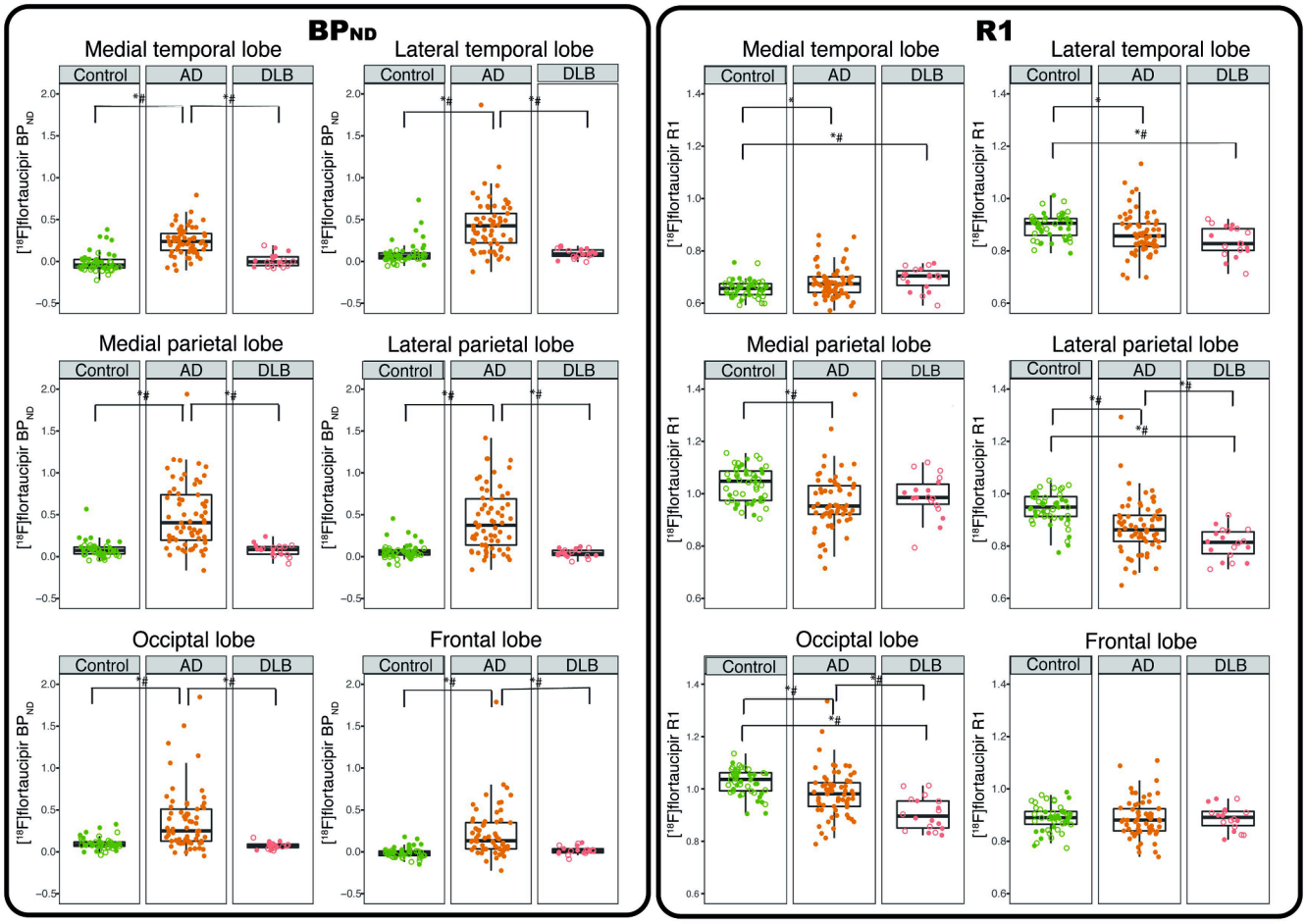


**Fig. 2.** Regional [$^{18}$F]flortaucipir $BP_{ND}$ (left) and $R_1$ (right) across dementia with Lewy bodies (DLB), Alzheimer's disease (AD) and controls for medial and lateral temporal/ parietal, occipital and frontal ROIs. The dots indicate the individual mean values within the diagnostic groups. Open dots are Aβ- subjects and closed dots are Aβ+ subjects. The box ranges from the first to the third quartile and the whiskers indicate the range from the minimum to quartile 1 and from quartile 3 to the maximum, excluding outliers. * $p_{uncorrected} < 0.05$.# $p_{Bonferroni} < 0.05$.

patients, which was in the same range as the controls. This is largely in line with other results (Nedelska et al., 2019; Smith et al., 2018a), whereas some studies reported higher tau uptake (Gomperts et al., 2016; Kantarci et al., 2017; Lee et al., 2018; Mak et al., 2019; Ossenkoppele et al., 2018), mainly in the occipital lobe (Kantarci et al., 2017; Lee et al., 2018; Mak et al., 2019). This discrepancy might be due to the difference in patient selection and disease severity as the DLB patients in the present study were more mildly affected (mean MMSE: 25 vs. 20–24 (Gomperts et al., 2016; Kantarci et al., 2017; Lee et al., 2018)). Additionally, in contrast to previous studies, we also included MCI-LB (Donaghy et al., 2015; van de Beek et al., 2020) which may have decreased the amount of tau observed. Similar to AD (Cho et al., 2019; Hanseeuw et al., 2019; Johnson et al., 2016a; Ossenkoppele et al., 2018; Sperling et al., 2019), the amount of [$^{18}$F]flortaucipir in DLB likely depends on clinical disease severity. Another explanation is that we studied a well-defined cohort of DLB patients, including DAT-SPECT as a supportive biomarker and we used extensive tests for characterizing the neuropsychological profile and clinical core features. We hereby minimized the risk of misdiagnosing DLB for AD, which show in general higher [$^{18}$F]flortaucipir retention levels than DLB patients (Kantarci et al., 2017; Lee et al., 2018; Ossenkoppele et al., 2018; Smith et al., 2018a). In addition, the amount of tau pathology may differ per clinical subtype of DLB (Ferman et al., 2020). Hence, it is conceivable our sample consisted mainly of a low tau subtypes of DLB.

Next, the amount of DLB-AD+ in our study was lower (mean = 33%) than in other studies (mean ~ 50%) which showed more tau uptake (Kantarci et al., 2017; Lee et al., 2018; Mak et al., 2019; Ossenkoppele et al., 2018). The presence of amyloid/ AD pathology may be related to increased [$^{18}$F]flortaucipir uptake in DLB patients, as suggested by our study (supplementary Fig. 1 and supplementary Table 1) and as previously described (Kantarci et al., 2017; Lee et al., 2018). Nevertheless, some studies also observed high tau uptake in DLB patients without evidence of amyloid pathology (Gomperts et al., 2016). Longitudinal studies are necessary to determine whether the presence of amyloid pathology is necessary for tau to spread in DLB, similar to what has been suggested in AD (Hanseeuw et al., 2019; Jacobs et al., 2018; Mattsson-Carlgren et al., 2020). Finally, we compared our DLB patients to SCD subjects which we used as controls and in line with literature (Jansen et al., 2015) ~40% of the controls with SCD had evidence for AD pathology. This may have influenced our results, however it was comparable to DLB-AD+ (Aβ+ 40% vs. 33%) and when we repeated our regional [$^{18}$F]flortaucipir $BP_{ND}$ analysis and compared the $BP_{ND}$ values of DLB patients to controls with SCD without AD pathology, we found comparable results (supplementary Table 5, supplementary Fig. 5). However, for the ROC curves (supplementary Fig. 5), both medial and lateral temporal [$^{18}$F]flortaucipir $BP_{ND}$ were best in distinguishing DLB from Aβ- controls (AUCs ≈ 0.8) compared to the frontal $BP_{ND}$ (AUC ≈0.7). for all controls (both Aβ+ and Aβ-). This difference is probably due to the age related tau deposition in Aβ+ controls (Johnson et al., 2016b; Pontecorvo et al., 2017; Scholl et al., 2016; Tosun et al., 2017) and the presence of Aβ may even induce tau to spread outside of the MTL (Jacobs et al., 2018; Ziontz et al., 2019). Therefore there may be an

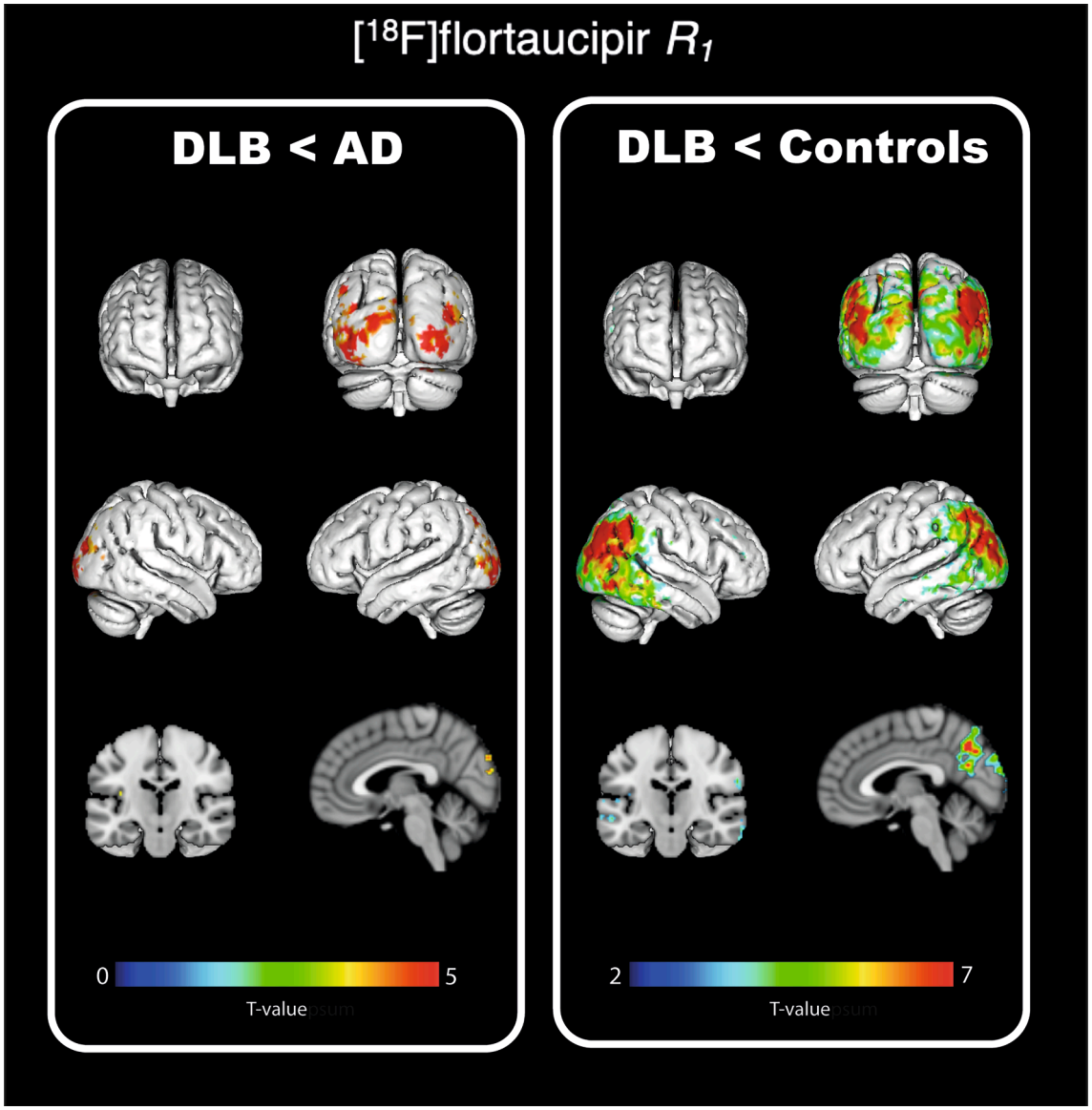


**Fig. 3.** Voxel-wise comparison of [$^{18}$F]flortaucipir $R_1$ images between dementia with Lewy body (DLB) versus Alzheimer's disease (left) and controls (right, $P_{uncorrected} < 0.001$).

increase in the diagnostic performance of [$^{18}$F]flortaucipir $BP_{ND}$ in DLB vs. Aβ- controls compared to both Aβ- and Aβ+ controls and this may explain the larger differences found between DLB patients and controls in other studies who used Aβ- controls (Gomperts et al., 2016; Lee et al., 2018).

We found lower parietal and occipital $R_1$ in DLB vs AD or controls and these regional rCBF differences were best in discriminating DLB from AD and controls (Fig. 4C–D). The rCBF spatial pattern of the present study is closely resembling [$^{18}$F]FDG parieto-occipital hypometabolism in DLB reported in previous studies (Albin et al., 1996; Higuchi et al., 2000; Imamura et al., 1997; Ishii et al., 1998; Kantarci et al., 2012; Klein et al., 2010; Liu et al., 2017; Minoshima et al., 1997) and the ability of occipital hypometabolism to distinguish DLB from AD (AUC = 0.80 – 0.86) (O'Brien et al., 2014). This was expected, since we and others observed a strong association between regional rCBF and [$^{18}$F]FDG metabolism, supporting the use of rCBF as a proxy of neuronal activity (Ottoy et al., 2019; Peretti et al., 2019; Rodriguez-Vieitez et al., 2016). However, we did not observe significant correlations between regional glucose metabolism and rCBF in the medial parietal (posterior cingulate) and temporal lobe. In DLB, metabolism in the medial temporal and posterior cingulate is relative spared (Morbelli et al., 2019), which could explain the non-significant associations in the present study.

We furthermore investigated whether tau PET or changes in rCBF were related to clinical characteristics. First, we found that both tau pathology and rCBF were not related to the clinical core features of DLB, which is largely in line with previous studies (Kantarci et al., 2017; Lee et al., 2018; Lobotesis et al., 2001; Nedelska et al., 2018). Although rCBF and [$^{18}$F]FDG metabolism are strongly related, a previous study in a large cohort of 171 DLB patients did find that hypometabolism was associated with worse clinical core features: fluctuations, hallucinations, parkinsonism and RBD (Morbelli et al., 2019). This discrepancy with our rCBF findings may be due to the larger sample size or difference in disease severity in that study, since hypometabolism patterns are highly affected by disease severity (Iizuka et al., 2017; Morbelli et al., 2019).

Second, we observed that rCBF, but not tau PET was related to cognitive impairment. This suggests that in our sample AD tau pathology plays a minor role in cognitive impairment observed in DLB, consistent with the majority of the previous [$^{18}$F]flortaucipir studies in DLB which did not find a relationship between tau PET and global cognition

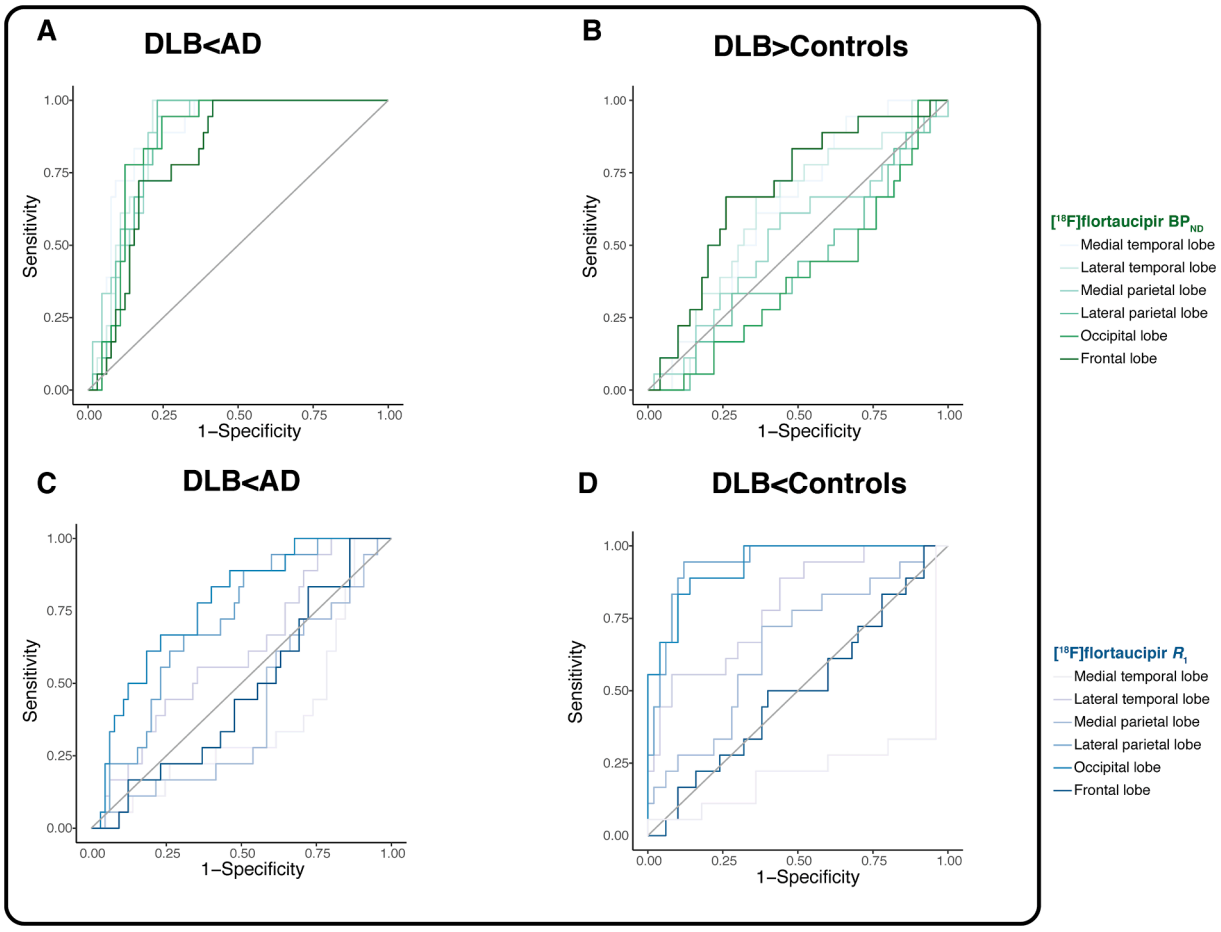


**Fig. 4.** Receiver operating curves for medial and lateral temporal/ parietal, occipital and frontal [$^{18}$F]flortaucipir $BP_{ND}$ (A-B) and $R_1$ (C-D) for distinguishing DLB from AD (A, C) and controls (B, D).

(Kantarci et al., 2017; Lee et al., 2018; Smith et al., 2018a). However, others did show an association between parietal tau PET and tests for fluency, but included a limited sample size (Smith et al., 2018a). In addition, neuropathological studies show consistent evidence for an important role of AD tau pathology in explaining the clinical variability of DLB (Ferman et al., 2020; Howlett et al., 2015; Irwin et al., 2017, 2018; Lemstra et al., 2017), however typically include more advanced DLB patients. The lack of relationships between tau pathology and clinical symptomatology may be explained by our sample consisting for a substantial part of MCI-LB. It is also possible that, contrary to AD, where the amount of tau is strongly associated to cognitive symptoms (Ossenkoppele et al., 2016, 2019), other pathologies, such as alpha-synuclein and neurotransmitter deficiencies, are more likely to be responsible for the majority of the cognitive symptoms in DLB. Indeed, rCBF, a surrogate marker for neuronal activity, was related to cognitive impairment in the present study. More specifically, in line with a previous [$^{18}$F]FDG PET study (Iizuka and Kameyama, 2016), we found that lower parietal rCBF was associated to lower scores on both immediate and delayed recall. In comparison to AD, DLB is characterized by more severe deficits in visuoperceptual, attentional and executive functioning (Metzler-Baddeley, 2007). We found that lower parietal and occipital rCBF were related to lower scores on visuospatial tasks: number locations (medial parietal rCBF) and fragmented letters (both lateral parietal and occipital rCBF). Furthermore, frontal rCBF was positively associated with digit span forward, an attention task. These results suggest that lower rCBF may be reflecting functional neuronal damage which is responsible for the clinical presentation of DLB. We previously found that lower rCBF was, independently of tau uptake, related to worse cognitive impairment across multiple cognitive domains (Visser et al., 2020), suggesting that rCBF may be of clinical importance in multiple neurodegenerative diseases. However, the associations between rCBF and cognition are subtle and did not survive correction for multiple comparison and therefore these results need to be replicated in larger cohorts and interpreted with caution. We found however, minimal additional value for the use a dynamic [$^{18}$F]flortaucipir PET to extract both tau binding and rCBF, when compared to [$^{18}$F]FDG PET alone.

### 4.1. *Strengths and limitations*

A strength of this study is that we used dynamic tau PET scans resulting in two measures: $BP_{ND}$ (tau binding) and $R_1$ (a proxy for rCBF). This enables us to derive a specific measurement of tau binding and a more general measurement related to hypometabolism at the same time. In this study we use $BP_{ND}$ to measure tau binding, which is a more specific measurement for tau binding than SUVr, which may overestimate true tracer binding. However, we found comparable associations for DLB and clinical outcomes when we replaced $BP_{ND}$ by SUVr and the mean $SUVr_{80\text{-}100min}$ image of DLB patients in the present study (supplementary Fig. 3) is comparable to previous studies (Smith et al., 2018a). A third strength of our study is that we were able to explore the influence of clinical DLB stage on the amount of [$^{18}$F]flortaucipir $BP_{ND}$ and $R_1$ within DLB (Supplementary Table 3).

A limitation of this study is the relatively small sample size, which may have hampered the detection of associations between PET measures and clinical characteristics of DLB and has the potential to over-fit the obtained ROC curves. Further limitations of this study include the lack of evidence on the neuropathological correlations of ante and postmortem [$^{18}$F]flortaucipir in DLB. Therefore, we cannot exclude that the

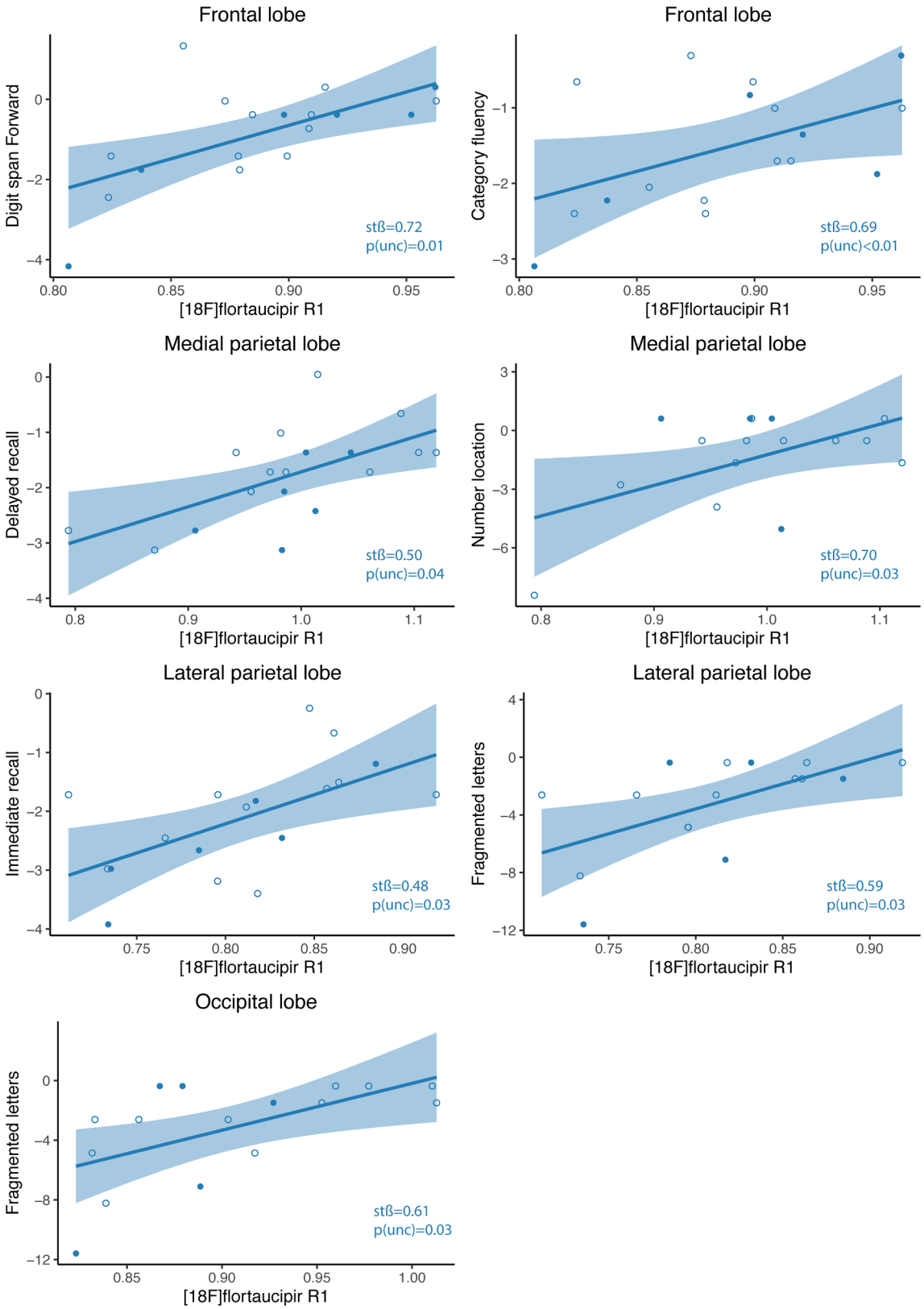


**Fig. 5.** Scatterplots of the observed relationship between frontal, medial / lateral parietal and occipital [$^{18}$F]flortaucipir $R_1$ and cognition in DLB. Each symbol represents one subject. Open circles are Aβ- subjects and closed circles are Aβ+ subjects Displayed are uncorrected p-values and additional # for Bonferroni correction for multiple comparison.

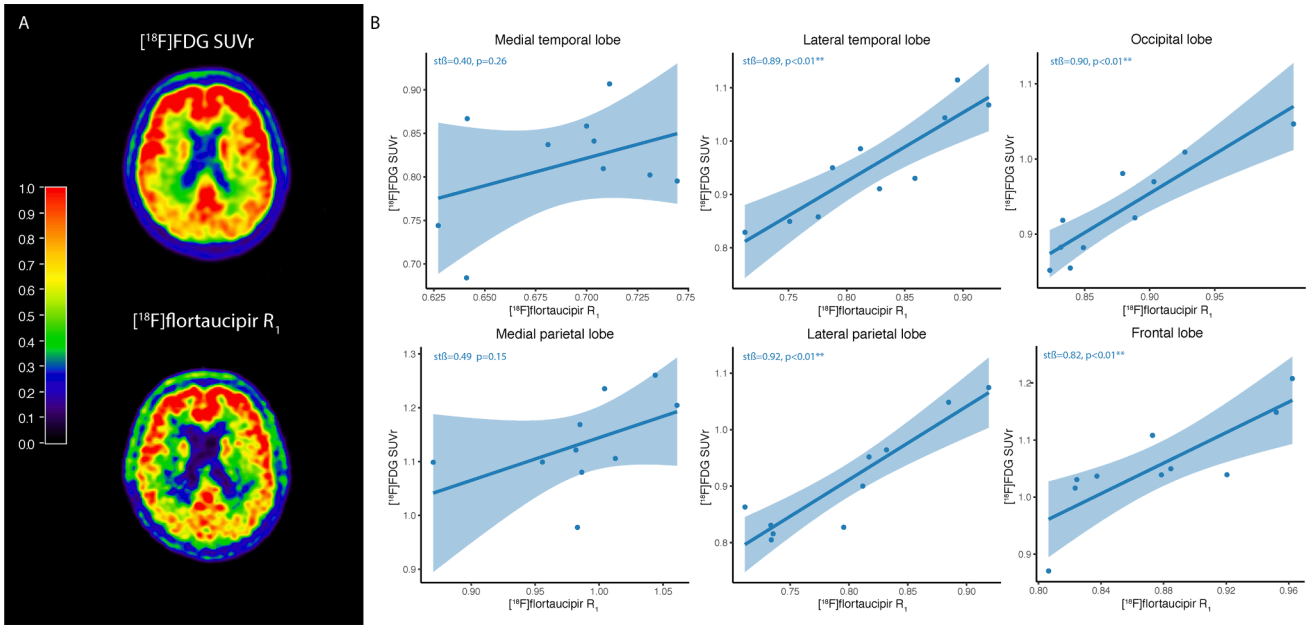


**Fig. 6.** Panel A representative image of a [$^{18}$F]FDG SUVr image (top row) and parametric [$^{18}$F]flortaucipir $R_1$ image (bottom row) and Panel B scatterplots of the observed relationship between [$^{18}$F]FDG SUVr with [$^{18}$F]flortaucipir $R_1$ within the medial/ lateral temporal/ parietal, occipital and frontal lobe in a subselection of the DLB patients (n = 10). Each symbol represents one subject. **p < 0.01.

possibility that the signal we observe is from other targets than tau. Notwithstanding, previous studies did show that [$^{18}$F]flortaucipir binds with high affinity to AD PHFs of tau, not to alpha-synuclein proteins and to a lesser extent to non– tau pathology (Lowe et al., 2016; Marquie et al., 2015). Third, we used a cross-sectional design and further studies with longitudinal tau PET data are required to explain the influence of AD tau pathology on the prognosis of DLB. Fourth, we did not include visual reads for the direct comparison between DLB patients and AD patients or controls. Although methods for the visual reads of AD are recently developed (Fleisher et al., 2020), there are currently no training programs for nuclear physicians and for this reason visual reading cannot be used as a clinical routine yet. Future research should focus on developing training programs for visual reads of [$^{18}$F]flortaucipir PET. Furthermore, $R_1$ is considered as relative flow distribution (relative to the cerebellar grey matter), but it has not been validated against the gold standard [$^{15}$O]$H_2O$. Notwithstanding, for other tracers such as [$^{11}$C]PIB (Chen et al., 2015) and [$^{18}$F]Florbetapir (Ottoy et al., 2019), $R_1$ was significantly associated with [$^{15}$O]$H_2O$ estimates (relative to the cerebellum). It is therefore reasonable to assume that $R_1$ of [$^{18}$F]flortaucipir may be used as surrogate for relative flow, but validation is warranted. Pending this validation, these results suggest that $R_1$ may be used to represent relative flow distribution in an AD cohort with cerebellar grey matter as reference region.

## 5. Conclusion

In our sample, tau PET in patients with DLB did not differ from controls and was not related to clinical features of DLB. Tau binding was slightly higher in DLB-AD+ compared to DLB-AD- patients. Contrary to tau, there were DLB-specific occipital and lateral parietal relative cerebral blood flow reductions compared to both controls and AD patients and lower regional rCBF was related to cognitive impairment. This indicates that assessment of rCBF may give more insight into disease mechanisms in DLB than tau PET.

## Declaration of interest

Wolters, van de Beek, Ossenkoppele, Golla, Verfaillie, Coomans, Timmers, Visser, Tuncel, Boellaard, Windhorst and Lemstra declares that he/she has no conflict of interest.

Van der Flier received grant support from ZonMW, NWO, EU-FP7, Alzheimer Nederland, CardioVascular Onderzoek Nederland, Stichting Dioraphte, Gieskes-Strijbis Fonds, Boehringer Ingelheim, Piramal Neuroimaging, Roche BV, Janssen Stellar, Combinostics. All funding is paid to the institution. WvdF holds the Pasman chair.

Van Berckel receives research support from ZON-MW, AVID radiopharmaceuticals, CTMM and Janssen Pharmaceuticals. He is a trainer for Piramal and GE. He receives no personal honoraria.

Barkhof is editorial board member of Brain, European Radiology, Neurology®, Multiple Sclerosis Journal, and Radiology; performed consultancy and received personal compensation and honoraria from Bayer-Schering Pharma and Genzyme; received compensation (personal and to institution) and honoraria from Biogen-IDEC, TEVA, Merck-Serono, Novartis, Roche, Synthon BV, and Jansen Research; received payment for development of educational presentations from IXICO and Biogen-IDEC (to institution); is funded by a Dutch MS Society grant, EU-FP7/H2020; and is supported by the NIH Research Biomedical Research Center at University College London Hospital.

Scheltens received grant support (to the institution) from GE Healthcare, Danone Research, Piramal and MERCK. In the past 2 years he has received consultancy/speaker fees from Lilly, GE Healthcare, Novartis, Forum, Sanofi, Nutricia, Probiodrug and EIP Pharma. All funding is paid to the institution.

No other potential conflicts of interest relevant to this article exist.

*Acknowledgments*

We kindly thank all participants for their contribution. Research of Amsterdam Alzheimer Center is part of the Neurodegeneration program of Amsterdam Neuroscience. The Amsterdam Alzheimer Center is supported by Alzheimer Nederland and Stichting VUmc funds. [$^{18}$F]Flortaucipir PET scans were made possible by Avid Radiopharmaceuticals Inc.

Financial disclosure: This research was funded by a ZonMW Memorabel grant. FB is supported by the NIHR biomedical research centre at UCLH.

## Appendix A. Supplementary data

Supplementary data to this article can be found online at https://doi.org/10.1016/j.nicl.2020.102504.

## References


Albert, M.S., DeKosky, S.T., Dickson, D., Dubois, B., Feldman, H.H., Fox, N.C., Gamst, A., Holtzman, D.M., Jagust, W.J., Petersen, R.C., 2011. The diagnosis of mild cognitive impairment due to Alzheimer's disease: Recommendations from the National Institute on Aging-Alzheimer's Association workgroups on diagnostic guidelines for Alzheimer's disease. Alzheimer's & dementia 7, 270–279.

Albin, R.L., Minoshima, S., D'Amato, C.J., Frey, K.A., Kuhl, D.A., Sima, A.A., 1996. Fluoro-deoxyglucose positron emission tomography in diffuse Lewy body disease. Neurology 47, 462–466.

Armstrong, M.J., Litvan, I., Lang, A.E., Bak, T.H., Bhatia, K.P., Borroni, B., Boxer, A.L., Dickson, D.W., Grossman, M., Hallett, M., Josephs, K.A., Kertesz, A., Lee, S.E., Miller, B.L., Reich, S.G., Riley, D.E., Tolosa, E., Troster, A.I., Vidailhet, M., Weiner, W.J., 2013. Criteria for the diagnosis of corticobasal degeneration. Neurology 80, 496–503.

Binnewijzend, M.A., Kuijer, J.P., van der Flier, W.M., Benedictus, M.R., Moller, C.M., Pijnenburg, Y.A., Lemstra, A.W., Prins, N.D., Wattjes, M.P., van Berckel, B.N., Scheltens, P., Barkhof, F., 2014. Distinct perfusion patterns in Alzheimer's disease, frontotemporal dementia and dementia with Lewy bodies. Eur. Radiol. 24, 2326–2333.

Boeve, B.F., Molano, J.R., Ferman, T.J., Smith, G.E., Lin, S.-C., Bieniek, K., Haidar, W., Tippmann-Peikert, M., Knopman, D.S., Graff-Radford, N.R., 2011. Validation of the Mayo Sleep Questionnaire to screen for REM sleep behavior disorder in an aging and dementia cohort. Sleep Med. 12, 445–453.

Chen, Y.J., Rosario, B.L., Mowrey, W., Laymon, C.M., Lu, X., Lopez, O.L., Klunk, W.E., Lopresti, B.J., Mathis, C.A., Price, J.C., 2015. Relative 11C-PiB Delivery as a Proxy of Relative CBF: Quantitative Evaluation Using Single-Session 15O-Water and 11C-PiB PET. J. Nucl. Med. 56, 1199–1205.

Cho, H., Choi, J.Y., Lee, H.S., Lee, J.H., Ryu, Y.H., Lee, M.S., Jack Jr., C.R., Lyoo, C.H., 2019. Progressive Tau Accumulation in Alzheimer Disease: 2-Year Follow-up Study. J. Nucl. Med. 60, 1611–1621.

Colloby, S.J., Fenwick, J.D., Williams, E.D., Paling, S.M., Lobotesis, K., Ballard, C., McKeith, I., O'Brien, J.T., 2002. A comparison of (99m)Tc-HMPAO SPET changes in dementia with Lewy bodies and Alzheimer's disease using statistical parametric mapping. Eur. J. Nucl. Med. Mol. Imaging 29, 615–622.

Crutch, S.J., Lehmann, M., Schott, J.M., Rabinovici, G.D., Rossor, M.N., Fox, N.C., 2012. Posterior cortical atrophy. Lancet Neurol. 11, 170–178.

de Wilde, A., van Maurik, I.S., Kunneman, M., Bouwman, F., Zwan, M., Willemse, E.A., Biessels, G.J., Minkman, M., Pel, R., Schoonenboom, N.S., Smets, E.M., Wattjes, M. P., Barkhof, F., Stephens, A., van Lier, E.J., Batrla-Utermann, R., Scheltens, P., Teunissen, C.E., van Berckel, B.N., van der Flier, W.M., 2017. Alzheimer's biomarkers in daily practice (ABIDE) project: Rationale and design. Alzheimers Dement (Amst) 6, 143–151.

Donaghy, P.C., O'Brien, J.T., Thomas, A.J., 2015. Prodromal dementia with Lewy bodies. Psychol. Med. 45, 259–268.

Dugger, B.N., Adler, C.H., Shill, H.A., Caviness, J., Jacobson, S., Driver-Dunckley, E., Beach, T.G., Disease, A.P., C.,, 2014. Concomitant pathologies among a spectrum of parkinsonian disorders. Parkinsonism Relat Disord 20, 525–529.

Duits, F.H., Teunissen, C.E., Bouwman, F.H., Visser, P.J., Mattsson, N., Zetterberg, H., Blennow, K., Hansson, O., Minthon, L., Andreasen, N., Marcusson, J., Wallin, A., Rikkert, M.O., Tsolaki, M., Parnetti, L., Herukka, S.K., Hampel, H., De Leon, M.J., Schroder, J., Aarsland, D., Blankenstein, M.A., Scheltens, P., van der Flier, W.M., 2014. The cerebrospinal fluid "Alzheimer profile": easily said, but what does it mean? Alzheimers Dement 10 (713–723), e712.

Ferman, T.J., Aoki, N., Boeve, B.F., Aakre, J.A., Kantarci, K., Graff-Radford, J., Parisi, J. E., Van Gerpen, J.A., Graff-Radford, N.R., Uitti, R.J., Pedraza, O., Murray, M.E., Wszolek, Z.K., Reichard, R.R., Fields, J.A., Ross, O.A., Knopman, D.S., Petersen, R.C., Dickson, D.W., 2020. Subtypes of dementia with Lewy bodies are associated with alpha-synuclein and tau distribution. Neurology 95, e155–e165.

Fleisher, A.S., Pontecorvo, M.J., Devous Sr., M.D., Lu, M., Arora, A.K., Truocchio, S.P., Aldea, P., Flitter, M., Locascio, T., Devine, M., Siderowf, A., Beach, T.G., Montine, T. J., Serrano, G.E., Curtis, C., Perrin, A., Salloway, S., Daniel, M., Wellman, C., Joshi, A.D., Irwin, D.J., Lowe, V.J., Seeley, W.W., Ikonomovic, M.D., Masdeu, J.C., Kennedy, I., Harris, T., Navitsky, M., Southekal, S., Mintun, M.A., Investigators, A.S., 2020. Positron Emission Tomography Imaging With [18F]flortaucipir and Postmortem Assessment of Alzheimer Disease Neuropathologic Changes. JAMA Neurol.

Folstein, M.F., Folstein, S.E., McHugh, P.R., 1975. "Mini-mental state". A practical method for grading the cognitive state of patients for the clinician. J. Psychiatr. Res. 12, 189–198.

Fong, T.G., Inouye, S.K., Dai, W., Press, D.Z., Alsop, D.C., 2011. Association cortex hypoperfusion in mild dementia with Lewy bodies: a potential indicator of cholinergic dysfunction? Brain Imaging Behav 5, 25–35.

Goetz, C.G., Tilley, B.C., Shaftman, S.R., Stebbins, G.T., Fahn, S., Martinez-Martin, P., Poewe, W., Sampaio, C., Stern, M.B., Dodel, R., 2008. Movement Disorder Society-sponsored revision of the Unified Parkinson's Disease Rating Scale (MDS-UPDRS): scale presentation and clinimetric testing results. Movement disorders: official journal of the Movement Disorder Society 23, 2129–2170.

Golla, S.S., Verfaillie, S.C., Boellaard, R., Adriaanse, S.M., Zwan, M.D., Schuit, R.C., Timmers, T., Groot, C., Schober, P., Scheltens, P., van der Flier, W.M., Windhorst, A. D., van Berckel, B.N., Lammertsma, A.A., 2018a. Quantification of [(18)F] florbetapir: A test-retest tracer kinetic modelling study. J Cereb Blood Flow Metab, 271678X18783628.

Golla, S.S., Wolters, E.E., Timmers, T., Ossenkoppele, R., van der Weijden, C.W., Scheltens, P., Schwarte, L., Mintun, M.A., Devous Sr., M.D., Schuit, R.C., Windhorst, A.D., Lammertsma, A.A., Yaqub, M., van Berckel, B.N., Boellaard, R., 2018. Parametric methods for [(18)F]flortaucipir PET. J. Cereb. Blood Flow Metab. 271678X18820765.

Golla, S.S.V., Timmers, T., Ossenkoppele, R., Groot, C., Verfaillie, S., Scheltens, P., van der Flier, W.M., Schwarte, L., Mintun, M.A., Devous, M., Schuit, R.C., Windhorst, A. D., Lammertsma, A.A., Boellaard, R., van Berckel, B.N.M., Yaqub, M., 2017. Quantification of Tau Load Using [18F]AV1451 PET. Mol Imaging Biol 19, 963–971.

Gomperts, S.N., Locascio, J.J., Makaretz, S.J., Schultz, A., Caso, C., Vasdev, N., Sperling, R., Growdon, J.H., Dickerson, B.C., Johnson, K., 2016. Tau Positron Emission Tomographic Imaging in the Lewy Body Diseases. JAMA Neurol 73, 1334–1341.

Gorno-Tempini, M.L., Hillis, A.E., Weintraub, S., Kertesz, A., Mendez, M., Cappa, S.F., Ogar, J.M., Rohrer, J.D., Black, S., Boeve, B.F., Manes, F., Dronkers, N.F., Vandenberghe, R., Rascovsky, K., Patterson, K., Miller, B.L., Knopman, D.S., Hodges, J.R., Mesulam, M.M., Grossman, M., 2011. Classification of primary progressive aphasia and its variants. Neurology 76, 1006–1014.

Goto, H., Ishii, K., Uemura, T., Miyamoto, N., Yoshikawa, T., Shimada, K., Ohkawa, S., 2010. Differential diagnosis of dementia with Lewy Bodies and Alzheimer Disease using combined MR imaging and brain perfusion single-photon emission tomography. AJNR Am. J. Neuroradiol. 31, 720–725.

Groot, C., van Loenhoud, A.C., Barkhof, F., van Berckel, B.N.M., Koene, T., Teunissen, C. C., Scheltens, P., van der Flier, W.M., Ossenkoppele, R., 2018. Differential effects of cognitive reserve and brain reserve on cognition in Alzheimer disease. Neurology 90, e149–e156.

Hammers, A., Allom, R., Koepp, M.J., Free, S.L., Myers, R., Lemieux, L., Mitchell, T.N., Brooks, D.J., Duncan, J.S., 2003. Three-dimensional maximum probability atlas of the human brain, with particular reference to the temporal lobe. Hum. Brain Mapp. 19, 224–247.

Hanseeuw, B.J., Betensky, R.A., Jacobs, H.I.L., Schultz, A.P., Sepulcre, J., Becker, J.A., Cosio, D.M.O., Farrell, M., Quiroz, Y.T., Mormino, E.C., Buckley, R.F., Papp, K.V., Amariglio, R.A., Dewachter, I., Ivanoiu, A., Huijbers, W., Hedden, T., Marshall, G.A., Chhatwal, J.P., Rentz, D.M., Sperling, R.A., Johnson, K., 2019. Association of Amyloid and Tau With Cognition in Preclinical Alzheimer Disease: A Longitudinal Study. JAMA Neurol.

Hanyu, H., Shimizu, S., Hirao, K., Kanetaka, H., Sakurai, H., Iwamoto, T., Koizumi, K., Abe, K., 2006. Differentiation of dementia with Lewy bodies from Alzheimer's disease using Mini-Mental State Examination and brain perfusion SPECT. J. Neurol. Sci. 250, 97–102.

Higuchi, M., Tashiro, M., Arai, H., Okamura, N., Hara, S., Higuchi, S., Itoh, M., Shin, R. W., Trojanowski, J.Q., Sasaki, H., 2000. Glucose hypometabolism and neuropathological correlates in brains of dementia with Lewy bodies. Exp. Neurol. 162, 247–256.

Howlett, D.R., Whitfield, D., Johnson, M., Attems, J., O'Brien, J.T., Aarsland, D., Lai, M. K., Lee, J.H., Chen, C., Ballard, C., Hortobagyi, T., Francis, P.T., 2015. Regional Multiple Pathology Scores Are Associated with Cognitive Decline in Lewy Body Dementias. Brain Pathol. 25, 401–408.

Iizuka, T., Iizuka, R., Kameyama, M., 2017. Cingulate island sign temporally changes in dementia with Lewy bodies. Sci. Rep. 7, 14745.

Iizuka, T., Kameyama, M., 2016. Cingulate island sign on FDG-PET is associated with medial temporal lobe atrophy in dementia with Lewy bodies. Ann. Nucl. Med. 30, 421–429.

Imamura, T., Ishii, K., Sasaki, M., Kitagaki, H., Yamaji, S., Hirono, N., Shimomura, T., Hashimoto, M., Tanimukai, S., Kazui, H., Mori, E., 1997. Regional cerebral glucose metabolism in dementia with Lewy bodies and Alzheimer's disease: a comparative study using positron emission tomography. Neurosci. Lett. 235, 49–52.

Irwin, D.J., Grossman, M., Weintraub, D., Hurtig, H.I., Duda, J.E., Xie, S.X., Lee, E.B., Van Deerlin, V.M., Lopez, O.L., Kofler, J.K., Nelson, P.T., Jicha, G.A., Woltjer, R., Quinn, J.F., Kaye, J., Leverenz, J.B., Tsuang, D., Longfellow, K., Yearout, D., Kukull, W., Keene, C.D., Montine, T.J., Zabetian, C.P., Trojanowski, J.Q., 2017. Neuropathological and genetic correlates of survival and dementia onset in synucleinopathies: a retrospective analysis. Lancet Neurol. 16, 55–65.

Irwin, D.J., Xie, S.X., Coughlin, D., Nevler, N., Akhtar, R.S., McMillan, C.T., Lee, E.B., Wolk, D.A., Weintraub, D., Chen-Plotkin, A., Duda, J.E., Spindler, M., Siderowf, A., Hurtig, H.I., Shaw, L.M., Grossman, M., Trojanowski, J.Q., 2018. CSF tau and beta-amyloid predict cerebral synucleinopathy in autopsied Lewy body disorders. Neurology 90, e1038–e1046.

Ishii, K., Imamura, T., Sasaki, M., Yamaji, S., Sakamoto, S., Kitagaki, H., Hashimoto, M., Hirono, N., Shimomura, T., Mori, E., 1998. Regional cerebral glucose metabolism in dementia with Lewy bodies and Alzheimer's disease. Neurology 51, 125–130.

Ishii, K., Yamaji, S., Kitagaki, H., Imamura, T., Hirono, N., Mori, E., 1999. Regional cerebral blood flow difference between dementia with Lewy bodies and AD. Neurology 53, 413–416.

Jacobs, H.I.L., Hedden, T., Schultz, A.P., Sepulcre, J., Perea, R.D., Amariglio, R.E., Papp, K.V., Rentz, D.M., Sperling, R.A., Johnson, K.A., 2018. Structural tract alterations predict downstream tau accumulation in amyloid-positive older individuals. Nat. Neurosci. 21, 424–431.

Jansen, W.J., Ossenkoppele, R., Knol, D.L., Tijms, B.M., Scheltens, P., Verhey, F.R.J., Visser, P.J., Aalten, P., Aarsland, D., Alcolea, D., Alexander, M., Almdahl, I.S., Arnold, S.E., Baldeiras, I., Barthel, H., van Berckel, B.N.M., Bibeau, K., Blennow, K.,

Brooks, D.J., van Buchem, M.A., Camus, V., Cavedo, E., Chen, K., Chetelat, G., Cohen, A.D., Drzezga, A., Engelborghs, S., Fagan, A.M., Fladby, T., Fleisher, A.S., van der Flier, W.M., Ford, L., Förster, S., Fortea, J., Foskett, N., Frederiksen, K.S., Freund-Levi, Y., Frisoni, G.B., Froelich, L., Gabryelewicz, T., Gill, K.D., Gkatzima, O., Gómez-Tortosa, E., Gordon, M.F., Grimmer, T., Hampel, H., Hausner, L., Hellwig, S., Herukka, S.-K., Hildebrandt, H., Ishihara, L., Ivanoiu, A., Jagust, W.J., Johannsen, P., Kandimalla, R., Kapaki, E., Klimkowicz-Mrowiec, A., Klunk, W.E., Köhler, S., Koglin, N., Kornhuber, J., Kramberger, M.G., Van Laere, K., Landau, S.M., Lee, D.Y., de Leon, M., Lisetti, V., Lleó, A., Madsen, K., Maier, W., Marcusson, J., Mattsson, N., de Mendonça, A., Meulenbroek, O., Meyer, P.T., Mintun, M.A., Mok, V., Molinuevo, J.L., Møllergård, H.M., Morris, J.C., Mroczko, B., Van der Mussele, S., Na, D.L., Newberg, A., Nordberg, A., Nordlund, A., Novak, G.P., Paraskevas, G.P., Parnetti, L., Perera, G., Peters, O., Popp, J., Prabhakar, S., Rabinovici, G.D., Ramakers, I.H.G.B., Rami, L., Resende de Oliveira, C., Rinne, J.O., Rodrigue, K.M., Rodríguez-Rodríguez, E., Roe, C.M., Rot, U., Rowe, C.C., Rüther, E., Sabri, O., Sanchez-Juan, P., Santana, I., Sarazin, M., Schröder, J., Schütte, C., Seo, S.W., Soetewey, F., Soininen, H., Spiru, L., Struyfs, H., Teunissen, C.E., Tsolaki, M., Vandenberghe, R., Verbeek, M.M., Villemagne, V.L., Vos, S.J.B., van Waalwijk van Doorn, L.J.C., Waldemar, G., Wallin, A., Wallin, Å.K., Wiltfang, J., Wolk, D.A., Zboch, M., Zetterberg, H.,, 2015. Prevalence of Cerebral Amyloid Pathology in Persons Without Dementia. JAMA 313, 1924.

Johnson, K.A., Schultz, A., Betensky, R.A., Becker, J.A., Sepulcre, J., Rentz, D., Mormino, E., Chhatwal, J., Amariglio, R., Papp, K., 2016a. Tau positron emission tomographic imaging in aging and early A lzheimer disease. Ann. Neurol. 79, 110–119.

Johnson, K.A., Schultz, A., Betensky, R.A., Becker, J.A., Sepulcre, J., Rentz, D., Mormino, E., Chhatwal, J., Amariglio, R., Papp, K., Marshall, G., Albers, M., Mauro, S., Pepin, L., Alverio, J., Judge, K., Philiossaint, M., Shoup, T., Yokell, D., Dickerson, B., Gomez-Isla, T., Hyman, B., Vasdev, N., Sperling, R., 2016b. Tau positron emission tomographic imaging in aging and early Alzheimer disease. Ann. Neurol. 79, 110–119.

Kantarci, K., Lowe, V.J., Boeve, B.F., Senjem, M.L., Tosakulwong, N., Lesnick, T.G., Spychalla, A.J., Gunter, J.L., Fields, J.A., Graff-Radford, J., Ferman, T.J., Jones, D.T., Murray, M.E., Knopman, D.S., Jack Jr., C.R., Petersen, R.C., 2017. AV-1451 tau and beta-amyloid positron emission tomography imaging in dementia with Lewy bodies. Ann. Neurol. 81, 58–67.

Kantarci, K., Lowe, V.J., Boeve, B.F., Weigand, S.D., Senjem, M.L., Przybelski, S.A., Dickson, D.W., Parisi, J.E., Knopman, D.S., Smith, G.E., Ferman, T.J., Petersen, R.C., Jack Jr., C.R., 2012. Multimodality imaging characteristics of dementia with Lewy bodies. Neurobiol. Aging 33, 2091–2105.

Klein, J.C., Eggers, C., Kalbe, E., Weisenbach, S., Hohmann, C., Vollmar, S., Baudrexel, S., Diederich, N.J., Heiss, W.D., Hilker, R., 2010. Neurotransmitter changes in dementia with Lewy bodies and Parkinson disease dementia in vivo. Neurology 74, 885–892.

Kosaka, K., 1978. Lewy bodies in cerebral cortex, report of three cases. Acta Neuropathol. 42, 127–134.

Kotzbauer, P.T., Tu, Z.D., Mach, R.H., 2017. Current status of the development of PET radiotracers for imaging alpha synuclein aggregates in Lewy bodies and Lewy neurites. Clin. Transl. Imaging 5, 3–14.

Landis, R., 2005. Standardized Regression Coefficients. Encyclopedia of Statistics in Behavioral Science. .

Lee, S.H., Cho, H., Choi, J.Y., Lee, J.H., Ryu, Y.H., Lee, M.S., Lyoo, C.H., 2018. Distinct patterns of amyloid-dependent tau accumulation in Lewy body diseases. Mov. Disord. 33, 262–272.

Lemstra, A.W., de Beer, M.H., Teunissen, C.E., Schreuder, C., Scheltens, P., van der Flier, W.M., Sikkes, S.A., 2017. Concomitant AD pathology affects clinical manifestation and survival in dementia with Lewy bodies. J. Neurol. Neurosurg. Psychiatry 88, 113–118.

Liu, S., Wang, X.D., Wang, Y., Shi, Z., Cai, L., Liu, S., Han, T., Zhou, Y., Wang, X., Gao, S., Ji, Y., 2017. Clinical and neuroimaging characteristics of Chinese dementia with Lewy bodies. PLoS ONE 12, e0171802.

Lobotesis, K., Fenwick, J.D., Phipps, A., Ryman, A., Swann, A., Ballard, C., McKeith, I.G., O'Brien, J.T., 2001. Occipital hypoperfusion on SPECT in dementia with Lewy bodies but not AD. Neurology 56, 643–649.

Lowe, V.J., Curran, G., Fang, P., Liesinger, A.M., Josephs, K.A., Parisi, J.E., Kantarci, K., Boeve, B.F., Pandey, M.K., Bruinsma, T., Knopman, D.S., Jones, D.T., Petrucelli, L., Cook, C.N., Graff-Radford, N.R., Dickson, D.W., Petersen, R.C., Jack Jr., C.R., Murray, M.E., 2016. An autoradiographic evaluation of AV-1451 Tau PET in dementia. Acta Neuropathol Commun 4, 58.

Mak, E., Surendranathan, A., Nicastro, N., Aigbirhio, F., Rowe, J., O'Brien, J., 2019. Imaging Tau, Neuroinflammation, and Abeta in Dementia With Lewy Bodies: A Deep-Phenotyping Case Report. Mov Disord Clin Pract 6, 77–80.

Marquie, M., Normandin, M.D., Meltzer, A.C., Siao Tick Chong, M., Andrea, N.V., Anton-Fernandez, A., Klunk, W.E., Mathis, C.A., Ikonomovic, M.D., Debnath, M., Bien, E.A., Vanderburg, C.R., Costantino, I., Makaretz, S., DeVos, S.L., Oakley, D.H., Gomperts, S.N., Growdon, J.H., Domoto-Reilly, K., Lucente, D., Dickerson, B.C., Frosch, M.P., Hyman, B.T., Johnson, K.A., Gomez-Isla, T., 2017. Pathological correlations of [F-18]-AV-1451 imaging in non-alzheimer tauopathies. Ann Neurol 81, 117-128.

Marquie, M., Normandin, M.D., Vanderburg, C.R., Costantino, I., Bien, E.A., Rycyna, L. G., Klunk, W.E., Mathis, C.A., Ikonomovic, M.D., Debnath, M.L., Vasdev, N., Dickerson, B.C., Gomperts, S.N., Growdon, J.H., Johnson, K.A., Frosch, M.P., Hyman, B.T., Gomez-Isla, T., 2015. Validating novel tau PET tracer [F-18]-AV-1451 (T807) on postmortem brain tissue. Ann. Neurol.

Mattsson-Carlgren, N., Andersson, E., Janelidze, S., Ossenkoppele, R., Insel, P., Strandberg, O., Zetterberg, H., Rosen, H.J., Rabinovici, G., Chai, X., Blennow, K., Dage, J.L., Stomrud, E., Smith, R., Palmqvist, S., Hansson, O., 2020. Aβ deposition is associated with increases in soluble and phosphorylated tau that precede a positive Tau PET in Alzheimer's disease. Science. Advances 6, eaaz2387.

McKeith, I.G., Boeve, B.F., Dickson, D.W., Halliday, G., Taylor, J.P., Weintraub, D., Aarsland, D., Galvin, J., Attems, J., Ballard, C.G., Bayston, A., Beach, T.G., Blanc, F., Bohnen, N., Bonanni, L., Bras, J., Brundin, P., Burn, D., Chen-Plotkin, A., Duda, J.E., El-Agnaf, O., Feldman, H., Ferman, T.J., Ffytche, D., Fujishiro, H., Galasko, D., Goldman, J.G., Gomperts, S.N., Graff-Radford, N.R., Honig, L.S., Iranzo, A., Kantarci, K., Kaufer, D., Kukull, W., Lee, V.M.Y., Leverenz, J.B., Lewis, S., Lippa, C., Lunde, A., Masellis, M., Masliah, E., McLean, P., Mollenhauer, B., Montine, T.J., Moreno, E., Mori, E., Murray, M., O'Brien, J.T., Orimo, S., Postuma, R.B., Ramaswamy, S., Ross, O.A., Salmon, D.P., Singleton, A., Taylor, A., Thomas, A., Tiraboschi, P., Toledo, J.B., Trojanowski, J.Q., Tsuang, D., Walker, Z., Yamada, M., Kosaka, K., 2017. Diagnosis and management of dementia with Lewy bodies: Fourth consensus report of the DLB Consortium. Neurology 89, 88–100.

McKeith, I.G., Ferman, T.J., Thomas, A.J., Blanc, F., Boeve, B.F., Fujishiro, H., Kantarci, K., Muscio, C., O'Brien, J.T., Postuma, R.B., Aarsland, D., Ballard, C., Bonanni, L., Donaghy, P., Emre, M., Galvin, J.E., Galasko, D., Goldman, J.G., Gomperts, S.N., Honig, L.S., Ikeda, M., Leverenz, J.B., Lewis, S.J.G., Marder, K.S., Masellis, M., Salmon, D.P., Taylor, J.P., Tsuang, D.W., Walker, Z., Tiraboschi, P., prodromal, D.L.B.D.S.G.,, 2020. Research criteria for the diagnosis of prodromal dementia with Lewy bodies. Neurology.

McKhann, G.M., Knopman, D.S., Chertkow, H., Hyman, B.T., Jack, C.R., Kawas, C.H., Klunk, W.E., Koroshetz, W.J., Manly, J.J., Mayeux, R., Mohs, R.C., Morris, J.C., Rossor, M.N., Scheltens, P., Carrillo, M.C., Thies, B., Weintraub, S., Phelps, C.H., 2011. The diagnosis of dementia due to Alzheimer's disease: recommendations from the National Institute on Aging-Alzheimer's Association workgroups on diagnostic guidelines for Alzheimer's disease. Alzheimers Dement 7, 263–269.

Metzler-Baddeley, C., 2007. A review of cognitive impairments in dementia with Lewy bodies relative to Alzheimer's disease and Parkinson's disease with dementia. Cortex 43, 583–600.

Minoshima, S., Giordani, B., Berent, S., Frey, K.A., Foster, N.L., Kuhl, D.E., 1997. Metabolic reduction in the posterior cingulate cortex in very early Alzheimer's disease. Ann. Neurol. 42, 85–94.

Morbelli, S., Chincarini, A., Brendel, M., Rominger, A., Bruffaerts, R., Vandenberghe, R., Kramberger, M.G., Trost, M., Garibotto, V., Nicastro, N., Frisoni, G.B., Lemstra, A.W., van der Zande, J., Pilotto, A., Padovani, A., Garcia-Ptacek, S., Savitcheva, I., Ochoa-Figueroa, M.A., Davidsson, A., Camacho, V., Peira, E., Arnaldi, D., Bauckneht, M., Pardini, M., Sambuceti, G., Aarsland, D., Nobili, F., 2019. Metabolic patterns across core features in dementia with lewy bodies. Ann. Neurol. 85, 715–725.

Nedelska, Z., Josephs, K.A., Graff-Radford, J., Przybelski, S.A., Lesnick, T.G., Boeve, B.F., Drubach, D.A., Knopman, D.S., Petersen, R.C., Jack Jr., C.R., Lowe, V.J., Whitwell, J. L., Kantarci, K., 2019. (18) F-AV-1451 uptake differs between dementia with lewy bodies and posterior cortical atrophy. Mov. Disord. 34, 344–352.

Nedelska, Z., Senjem, M.L., Przybelski, S.A., Lesnick, T.G., Lowe, V.J., Boeve, B.F., Arani, A., Vemuri, P., Graff-Radford, J., Ferman, T.J., Jones, D.T., Savica, R., Knopman, D.S., Petersen, R.C., Jack, C.R., Kantarci, K., 2018. Regional cortical perfusion on arterial spin labeling MRI in dementia with Lewy bodies: Associations with clinical severity, glucose metabolism and tau PET. Neuroimage Clin 19, 939–947.

O'Brien, J.T., Firbank, M.J., Davison, C., Barnett, N., Bamford, C., Donaldson, C., Olsen, K., Herholz, K., Williams, D., Lloyd, J., 2014. 18F-FDG PET and perfusion SPECT in the diagnosis of Alzheimer and Lewy body dementias. J. Nucl. Med. 55, 1959–1965.

Ossenkoppele, R., Pijnenburg, Y.A.L., Perry, D.C., Cohn-Sheehy, B.I., Scheltens, N.M.E., Vogel, J.W., Kramer, J.H., van der Vlies, A.E., La Joie, R., Rosen, H.J., van der Flier, W.M., Grinberg, L.T., Rozemuller, A.J., Huang, E.J., van Berckel, B.N.M., Miller, B.L., Barkhof, F., Jagust, W.J., Scheltens, P., Seeley, W.W., Rabinovici, G.D., 2015. The behavioural/dysexecutive variant of Alzheimer's disease: clinical, neuroimaging and pathological features. Brain : a journal of neurology 138, 2732–2749.

Ossenkoppele, R., Rabinovici, G.D., Smith, R., Cho, H., Scholl, M., Strandberg, O., Palmqvist, S., Mattsson, N., Janelidze, S., Santillo, A., Ohlsson, T., Jogi, J., Tsai, R., La Joie, R., Kramer, J., Boxer, A.L., Gorno-Tempini, M.L., Miller, B.L., Choi, J.Y., Ryu, Y.H., Lyoo, C.H., Hansson, O., 2018. Discriminative Accuracy of [18F] flortaucipir Positron Emission Tomography for Alzheimer Disease vs Other Neurodegenerative Disorders. JAMA 320, 1151–1162.

Ossenkoppele, R., Schonhaut, D.R., Scholl, M., Lockhart, S.N., Ayakta, N., Baker, S.L., O'Neil, J.P., Janabi, M., Lazaris, A., Cantwell, A., Vogel, J., Santos, M., Miller, Z.A., Bettcher, B.M., Vossel, K.A., Kramer, J.H., Gorno-Tempini, M.L., Miller, B.L., Jagust, W.J., Rabinovici, G.D., 2016. Tau PET patterns mirror clinical and neuroanatomical variability in Alzheimer's disease. Brain 139, 1551–1567.

Ossenkoppele, R., Smith, R., Ohlsson, T., Strandberg, O., Mattsson, N., Insel, P.S., Palmqvist, S., Hansson, O., 2019. Associations between tau, Abeta, and cortical thickness with cognition in Alzheimer disease. Neurology 92, e601–e612.

Ottoy, J., Verhaeghe, J., Niemantsverdriet, E., De Roeck, E., Wyffels, L., Ceyssens, S., Van Broeckhoven, C., Engelborghs, S., Stroobants, S., Staelens, S., 2019. (18)F-FDG PET, the early phases and the delivery rate of (18)F-AV45 PET as proxies of cerebral blood flow in Alzheimer's disease: Validation against (15)O-H2O PET. Alzheimers Dement 15, 1172–1182.

Pasquier, J., Michel, B.F., Brenot-Rossi, I., Hassan-Sebbag, N., Sauvan, R., Gastaut, J.L., 2002. Value of (99m)Tc-ECD SPET for the diagnosis of dementia with Lewy bodies. Eur. J. Nucl. Med. Mol. Imaging 29, 1342–1348.

Peretti, D.E., Vallez Garcia, D., Reesink, F.E., van der Goot, T., De Deyn, P.P., de Jong, B. M., Dierckx, R., Boellaard, R., 2019. Relative cerebral flow from dynamic PIB scans as an alternative for FDG scans in Alzheimer's disease PET studies. PLoS ONE 14, e0211000.

Pontecorvo, M.J., Devous Sr., M.D., Navitsky, M., Lu, M., Salloway, S., Schaerf, F.W., Jennings, D., Arora, A.K., McGeehan, A., Lim, N.C., Xiong, H., Joshi, A.D., Siderowf, A., Mintun, M.A., investigators, F.A.-A.,, 2017. Relationships between flortaucipir PET tau binding and amyloid burden, clinical diagnosis, age and cognition. Brain 140, 748–763.

Rodell, A.B., O'Keefe, G., Rowe, C.C., Villemagne, V.L., Gjedde, A., 2016. Cerebral Blood Flow and Abeta-Amyloid Estimates by WARM Analysis of [(11)C]PiB Uptake Distinguish among and between Neurodegenerative Disorders and Aging. Front. Aging Neurosci. 8, 321.

Rodriguez-Vieitez, E., Leuzy, A., Chiotis, K., Saint-Aubert, L., Wall, A., Nordberg, A., 2016. Comparability of [18F]THK5317 and [11C]PIB blood flow proxy images with [18F]FDG positron emission tomography in Alzheimer's disease. J. Cereb. Blood Flow Metab. 0271678X16645593.

Rossell, S.L., Schutte, M.J., Toh, W.L., Thomas, N., Strauss, C., Linszen, M.M., van Dellen, E., Heringa, S.M., Teunisse, R., Slotema, C.W., 2019. The questionnaire for psychotic experiences: an examination of the validity and reliability. Schizophr. Bull. 45, S78–S87.

Scholl, M., Lockhart, S.N., Schonhaut, D.R., O'Neil, J.P., Janabi, M., Ossenkoppele, R., Baker, S.L., Vogel, J.W., Faria, J., Schwimmer, H.D., Rabinovici, G.D., Jagust, W.J., 2016. PET Imaging of Tau Deposition in the Aging Human Brain. Neuron 89, 971–982.

Slot, R.E.R., Verfaillie, S.C.J., Overbeek, J.M., Timmers, T., Wesselman, L.M.P., Teunissen, C.E., Dols, A., Bouwman, F.H., Prins, N.D., Barkhof, F., Lammertsma, A. A., Van Berckel, B.N.M., Scheltens, P., Sikkes, S.A.M., Van der Flier, W.M., 2018. Subjective Cognitive Impairment Cohort (SCIENCe): study design and first results. Alzheimers Res Ther 10, 76.

Smith, R., Scholl, M., Londos, E., Ohlsson, T., Hansson, O., 2018a. (18)F-AV-1451 in Parkinson's Disease with and without dementia and in Dementia with Lewy Bodies. Sci. Rep. 8, 4717.

Smith, R., Wibom, M., Pawlik, D., Englund, E., Hansson, O., 2018b. Correlation of In Vivo [18F]Flortaucipir With Postmortem Alzheimer Disease Tau Pathology. JAMA Neurol.

Sperling, R.A., Mormino, E.C., Schultz, A.P., Betensky, R.A., Papp, K.V., Amariglio, R.E., Hanseeuw, B.J., Buckley, R., Chhatwal, J., Hedden, T., Marshall, G.A., Quiroz, Y.T., Donovan, N.J., Jackson, J., Gatchel, J.R., Rabin, J.S., Jacobs, H., Yang, H.S., Properzi, M., Kirn, D.R., Rentz, D.M., Johnson, K.A., 2019. The impact of amyloid-beta and tau on prospective cognitive decline in older individuals. Ann. Neurol. 85, 181–193.

Svarer, C., Madsen, K., Hasselbalch, S.G., Pinborg, L.H., Haugbol, S., Frokjaer, V.G., Holm, S., Paulson, O.B., Knudsen, G.M., 2005. MR-based automatic delineation of volumes of interest in human brain PET images using probability maps. NeuroImage 24, 969–979.

Taylor, J.P., Firbank, M.J., He, J., Barnett, N., Pearce, S., Livingstone, A., Vuong, Q., McKeith, I.G., O'Brien, J.T., 2012. Visual cortex in dementia with Lewy bodies: magnetic resonance imaging study. Br. J. Psychiatry 200, 491–498.

Tosun, D., Landau, S., Aisen, P.S., Petersen, R.C., Mintun, M., Jagust, W., Weiner, M.W., Neuroimaging, Alzheimer's Disease, I.,, 2017. Association between tau deposition and antecedent amyloid-beta accumulation rates in normal and early symptomatic individuals. Brain 140, 1499–1512.

van de Beek, M., van Steenoven, I., van der Zande, J.J., Barkhof, F., Teunissen, C.E., van der Flier, W.M., Lemstra, A.W., 2020. Prodromal Dementia with Lewy Bodies: Clinical Characterization and Predictors of Progression. Mov Disord.

van der Flier, W.M., Scheltens, P., 2018. Amsterdam Dementia Cohort: Performing Research to Optimize Care. J. Alzheimers Dis. 62, 1091–1111.

Verhage, F., 1964. Intelligence and age: study with Dutch people aged 12–77.

Visser, D., Wolters, E.E., Verfaillie, S.C.J., Coomans, E.M., Timmers, T., Tuncel, H., Reimand, J., Boellaard, R., Windhorst, A.D., Scheltens, P., van der Flier, W.M., Ossenkoppele, R., van Berckel, B.N.M., 2020. Tau pathology and relative cerebral blood flow are independently associated with cognition in Alzheimer's disease. Eur. J. Nucl. Med. Mol. Imaging.

Vollmar, S., Michel, C., Treffert, J.T., Newport, D.F., Casey, M., Knoss, C., Wienhard, K., Liu, X., Defrise, M., Heiss, W.D., 2002. HeinzelCluster: accelerated reconstruction for FORE and OSEM3D. Phys. Med. Biol. 47, 2651–2658.

Walker, M., Ayre, G., Cummings, J., Wesnes, K., McKeith, I., O'Brien, J., Ballard, C., 2000. The clinician assessment of fluctuation and the one day fluctuation assessment scale: two methods to assess fluctuating confusion in dementia. The British Journal of Psychiatry 177, 252–256.

Wolters, E.E., Golla, S.S.V., Timmers, T., Ossenkoppele, R., van der Weijden, C.W.J., Scheltens, P., Schwarte, L., Schuit, R.C., Windhorst, A.D., Barkhof, F., Yaqub, M., Lammertsma, A.A., Boellaard, R., van Berckel, B.N.M., 2018. A novel partial volume correction method for accurate quantification of [(18)F] flortaucipir in the hippocampus. EJNMMI Res 8, 79.

Ziontz, J., Bilgel, M., Shafer, A.T., Moghekar, A., Elkins, W., Helphrey, J., Gomez, G., June, D., McDonald, M.A., Dannals, R.F., Azad, B.B., Ferrucci, L., Wong, D.F., Resnick, S.M., 2019. Tau pathology in cognitively normal older adults. Alzheimers Dement (Amst) 11, 637–645.

Zwan, M.D., Ossenkoppele, R., Tolboom, N., Beunders, A.J., Kloet, R.W., Adriaanse, S.M., Boellaard, R., Windhorst, A.D., Raijmakers, P., Adams, H., Lammertsma, A.A., Scheltens, P., van der Flier, W.M., van Berckel, B.N., 2014. Comparison of simplified parametric methods for visual interpretation of 11C-Pittsburgh compound-B PET images. J. Nucl. Med. 55, 1305–1307.